

ORIGINAL RESEARCH ARTICLE



Hypertriglyceridemia as a Key Contributor to Abdominal Aortic Aneurysm Development and Rupture: Insights From Genetic and Experimental Models

Yaozhong Liu , MD; Huilun Wang, PhD; Minzhi Yu, PhD; Lei Cai , PhD; Ying Zhao , BS; Yalun Cheng, MD; Yongjie Deng , MD; Yang Zhao , PhD; Haocheng Lu , PhD; Xiaokang Wu , MD, PhD; Guizhen Zhao, PhD; Chao Xue , MD, PhD; Hongyu Liu, MD; Ida Surakka , PhD; Anna Schwendeman , PhD; Hong S. Lu , PhD; Alan Daugherty , PhD; Lin Chang , PhD; Jifeng Zhang , PhD; Ryan E. Temel, PhD; Y. Eugene Chen , MD, PhD; Yanhong Guo , MD, PhD

BACKGROUND: Abdominal aortic aneurysm (AAA) is a life-threatening vascular disease with no effective pharmacological treatments. The causal role of triglycerides (TGs) in AAA development remains unclear and controversial.

METHODS: Mendelian randomization was applied to assess causal relationships between lipoproteins, circulating proteins, metabolites, and the risk of AAA. To test the hypothesis that elevated plasma TG levels accelerate AAA development, we used *Lpl*-deficient, *Apoa5*-deficient, and human *APOC3* transgenic mice, which display varying degrees of hypertriglyceridemia. Mechanistic studies were performed using RNA sequencing and Western blot analysis of palmitate-treated vascular smooth muscle cells and validated *in vivo* by local overexpression of key mediator in the suprarenal abdominal aorta. Antisense oligonucleotides targeting *Angptl3* were administered to reduce TG levels and assess therapeutic potential in human *APOC3* transgenic and *Apoe*-deficient mice.

RESULTS: Mendelian randomization analyses integrating genetic, proteomic, and metabolomic data identified causal relationships between elevated TG-rich lipoproteins, TG metabolism-related proteins/metabolites, and AAA risk. In the angiotensin II infusion AAA model, most *Lpl*-deficient mice with severely elevated TG concentrations died of aortic rupture. Similarly, *Apoa5*-deficient mice with moderately elevated TG levels developed accelerated AAA, and human *APOC3* transgenic mice with dramatically elevated TG levels exhibited aortic dissection and rupture. Mechanistically, elevated TG and palmitate inhibited lysyl oxidase (LOX) maturation and reduced LOX activity. Locally overexpressing lysyl oxidase eliminated the proaneurysmal effect of hypertriglyceridemia in human *APOC3* transgenic mice. Moreover, an *Angptl3*-targeting antisense oligonucleotide profoundly attenuated AAA progression in both human *APOC3* transgenic and *Apoe*-deficient mice.

CONCLUSIONS: These findings identify hypertriglyceridemia as a key contributor to AAA pathogenesis and suggest that targeting TG-rich lipoproteins may be a promising therapeutic strategy for AAA.

Key Words: abdominal aortic aneurysm ■ lysyl oxidase ■ muscle, smooth, vascular ■ palmitate ■ triglycerides

Correspondence to: Yanhong Guo, MD, PhD, or Y. Eugene Chen, MD, PhD, Department of Internal Medicine, University of Michigan Medical Center, 1500 E Medical Center Dr, Ann Arbor, MI 48109, Email yanhongg@umich.edu or echenum@umich.edu; or Ryan E. Temel, PhD, Saha Cardiovascular Research Center and Department of Physiology, College of Medicine, University of Kentucky, 741 South Limestone, BBSRB B351, Lexington, KY 40536, Email ryan.temel@uky.edu
Supplemental Material is available with this article at <https://www.ahajournals.org/doi/suppl/10.1161/CIRCULATIONAHA.125.074737>.

Continuing medical education (CME) credit is available for this article. Go to <https://cme.ahajournals.org> to take the quiz.

For Sources of Funding and Disclosures, see page 879.

© 2025 American Heart Association, Inc.

Circulation is available at www.ahajournals.org/journal/circ

Clinical Perspective

What Is New?

- This study integrates genetic, proteomic, and metabolomic data to identify causation between increased triglyceride-rich lipoproteins and abdominal aortic aneurysm (AAA) risk.
- Triglyceride concentrations influence AAA formation and severity in a dose-dependent manner, potentially by inhibiting lysyl oxidase maturation and extracellular matrix assembly.
- Administration of an antisense oligonucleotide targeting *Angptl3* profoundly inhibits AAA progression in human *APOC3* transgenic mice and *Apoe*-deficient mice by lowering triglyceride concentrations.

What Are the Clinical Implications?

- These findings underscore triglyceride-rich lipoprotein management as a promising therapeutic strategy for AAA treatment.
- Antisense oligonucleotide therapy targeting liver *ANGPTL3* holds potential as a therapeutic approach to reduce AAA risk.

Abdominal aortic aneurysm (AAA) is a progressive vascular disease characterized by the localized enlargement of the abdominal aorta. The prevalence of AAA is estimated to be as high as 8% in men and 2% in women >65 years of age.¹ Most AAAs are asymptomatic, but the mortality rate is up to 80% if rupture occurs.² As the maximum aortic diameter is the most established predictor of aneurysm rupture, current guidelines recommend considering surgical repair for asymptomatic AAA patients when the maximal aortic diameter is ≥50 mm in women and ≥55 mm in men. Open surgical or percutaneous endovascular aneurysm repair is still the only therapeutic option.³ Patients with AAA smaller than these thresholds are typically monitored through imaging surveillance. AAA-relevant risk factors, including smoking, male sex, aging, hypertension, and hyperlipidemia, are associated with enhanced aneurysm formation and growth. Currently, medications to reduce AAA risk factors, such as angiotensin II (AngII) receptor antagonists, beta-adrenoceptor blockers, statins, and anticoagulants, have not been proven effective in halting the growth of an aneurysm or preventing the rupture of asymptomatic AAAs based on the findings from randomized controlled trials.^{4,5}

Our recent comprehensive genome-wide association study (GWAS) meta-analysis, which included ≈40 000 individuals with AAAs and >1 million individuals without AAAs, has demonstrated that one-third of the lead variants at the 121 genome-wide significant AAA risk loci are associated with major-lipid fractions, such as total cholesterol (TC), triglycerides (TGs), low-density lipopro-

Nonstandard Abbreviations and Acronyms

AAA	abdominal aortic aneurysm
ADAMTS2	a disintegrin and metalloproteinase with thrombospondin motif 2
AngII	angiotensin II
ANGPTL3	angiopoietin-like protein 3
APOA5	apolipoprotein A5
APOC3	apolipoprotein C-III
APOE	apolipoprotein E
ASO	antisense oligonucleotide
BMP-1	bone morphogenetic protein 1
BUPA	British United Provident Association
ECM	extracellular matrix
FAME-2	Fenofibrate in the Management of Abdominal Aortic Aneurysm 2
GFP	green fluorescent protein
GWAS	genome-wide association study
hAPOC3 Tg	human <i>APOC3</i> transgenic
HASMC	human aortic smooth muscle cell
HDL	high-density lipoprotein
LDL	low-density lipoprotein
LOX	lysyl oxidase
LPA	lipoprotein(a)
LPL	lipoprotein lipase
MR	Mendelian randomization
NEFA	nonesterified fatty acid
OE	overexpression
OR	odds ratio
PA	palmitic acid
PLTP	phospholipid transfer protein
RNA-seq	RNA sequencing
TC	total cholesterol
TG	triglyceride
TRL	TG-rich lipoprotein
VLDL	very low-density lipoprotein
WT	wild-type

tein cholesterol (LDL-C), or high-density lipoprotein cholesterol (HDL-C).⁶ Other genetic association studies have identified that a 1-SD increase in TG concentration is associated with a 69% higher risk of AAA.^{7,8} Population-based studies have reported that individuals with increased serum very low-density lipoprotein (VLDL) cholesterol and TG concentrations are more likely to develop larger AAAs and have a higher risk of rupture.^{9,10} These epidemiological and genetic findings suggest that increased TRLs (TG-rich lipoproteins) may accelerate AAA development and rupture, and modulating TG concentrations or metabolites may become new therapeutic strategies for AAA.

TGs, also known as triacylglycerols, are composed of glycerol and fatty acids and are the most abundant lipids in the body. Chylomicrons transport dietary TGs from the small intestine, and VLDLs transport endogenously synthesized TGs from the liver to peripheral tissues, such as the heart, skeletal muscle, and adipose tissues. TG metabolism is a complex process involving the breakdown and use of this lipid. Several proteins and enzymes play critical roles in regulating TG metabolism.¹¹ Among these, LPL (lipoprotein lipase), ApoC-III (apolipoprotein C-III, APOC3), ApoC-II, ApoA-V (apolipoprotein A5, APOA5), ANGPTL3, ANGPTL4, and ANGPTL8 (angiopoietin-like proteins) are key players. LPL is a critical enzyme that facilitates the hydrolysis of TGs carried by chylomicrons and VLDL into free fatty acids and glycerol, allowing them to be used by various cells for energy or storage. Our previous study found that an intronic LPL variant, associated with increased LPL expression, was strongly related to reduced plasma TG concentration and AAA risk.⁶ APOA5 is almost exclusively expressed in the liver and secreted in conjunction with VLDL particles. ApoC-III is a constituent of chylomicrons and VLDL particles and inhibits LPL activity, whereas ApoA-V and ApoC-II enhance LPL activity and promote the clearance of TG-rich lipoproteins. ANGPTL3 and ANGPTL8 are secreted proteins and inhibitors of LPL-mediated plasma TG clearance. In numerous studies involving humans and animals, loss of function of APOC2 or APOA5 is associated with increased plasma concentrations of TGs and chylomicronemia.^{12,13} Among the putatively causal circulating proteins associated with AAA, we identified that higher APOA5 expression is significantly associated with decreased AAA risk.⁶ Currently, gene silencing of APOC3 or ANGPTL3 significantly reduces TG and TC concentrations, making this method an effective strategy for lowering plasma lipids and preventing cardiovascular diseases.^{14–17} In the present study, we demonstrated that increased TG-rich lipoproteins accelerate AAA formation and rupture, and we provide evidence showing that effective management of plasma TG concentrations can alleviate AAA progression.

METHODS

The data, analytic methods, and code will be made available to other researchers from the corresponding author upon reasonable request for reproduction. A detailed description of the methods is available in the [Supplemental Material](#). All genetic data used in this study were obtained from publicly available consortiums. The original RNA sequencing (RNA-seq) data generated during this study were uploaded to the Gene Expression Omnibus (accession number GSE299480). All animal procedures followed the protocols approved by the institutional animal care and use committee at the University of Michigan (PRO00011743) and University of Kentucky (2023-4352).

Statistical Analysis

Analyses of RNA-seq and genetic data were performed using R language (version 4.3.0). Statistical analyses of other data were conducted using GraphPad Prism 10. Most of the data are presented as mean \pm SEM. The distribution of data was assessed using the Kolmogorov-Smirnov test (for $n>4$) or the Shapiro-Wilk test (for $n\leq 4$). For normally distributed data, Student *t* tests were used to compare 2 groups, 1-way ANOVA was used to compare multiple groups, and the Sidak method was applied for multiple comparisons correction. For non-normally distributed data, Mann-Whitney *U* tests were used to compare 2 groups, Kruskal-Wallis tests were employed to compare multiple groups, and the Dunn method was used for multiple comparisons correction. Two-way ANOVA followed by the Sidak correction was used to analyze experiments with 2 independent factors. Two-way mixed-effects ANOVA followed by the Sidak correction was used for experiments involving repeated measurements and multiple groups. $P<0.05$ was considered statistically significant.

RESULTS

Genetic, Proteomic, and Metabolic Studies Underscore High TG-Rich Lipoproteins as a Causal Risk Factor for AAA

Genetic variants that modulate the expression of genes encoding the candidate proteins or the abundance of metabolites are valuable tools for guiding therapeutic strategies. Recent studies have identified *cis*-acting protein quantitative trait loci that can be used as instrumental variables for inferring causality.^{18,19} Combining *cis*-acting protein quantitative trait locus and GWAS findings, we performed Mendelian randomization (MR) analyses to assess the causal effects of circulating proteins on AAA risk and identified that 41 of 2698 circulating proteins were significantly associated with AAA after adjusting for multiple tests (Figure 1A; full MR results in [Table S1](#)). Among them, genetically determined circulating APOC3 (odds ratio [OR], 1.84 [95% CI, 1.66–2.04]) and APOA5 (OR, 0.61 [95% CI, 0.56–0.67]) had the most significant effects on AAA risk. Seven of the 41 circulating proteins (APOC3, APOA5, LPL, APOE [apolipoprotein E], PLTP [phospholipid transfer protein], PCSK9 [proprotein convertase subtilisin/kexin type 9], and LPA [lipoprotein(a)]) play important roles in lipid metabolism, especially in VLDL and chylomicron metabolism (Figure 1B). Using multi-instrument variable MR to account for potential pleiotropy, 6 of the 7 lipid metabolism-related proteins (APOC3, LPL, APOE, PLTP, PCSK9, and LPA) were found to have causal effects on AAA across inverse-variance weighted MR, weighted median MR, and MR-Egger analyses ([Table S2](#)). Our previous GWAS findings demonstrated that 42 lead variants at the AAA risk loci are associated with major lipid fractions.⁶ After prioritizing the role of 5 major lipoprotein components (HDL-C, LDL-C, TG, APOA1 [apolipoprotein a1], and APOB [apolipoprotein B]) as risk

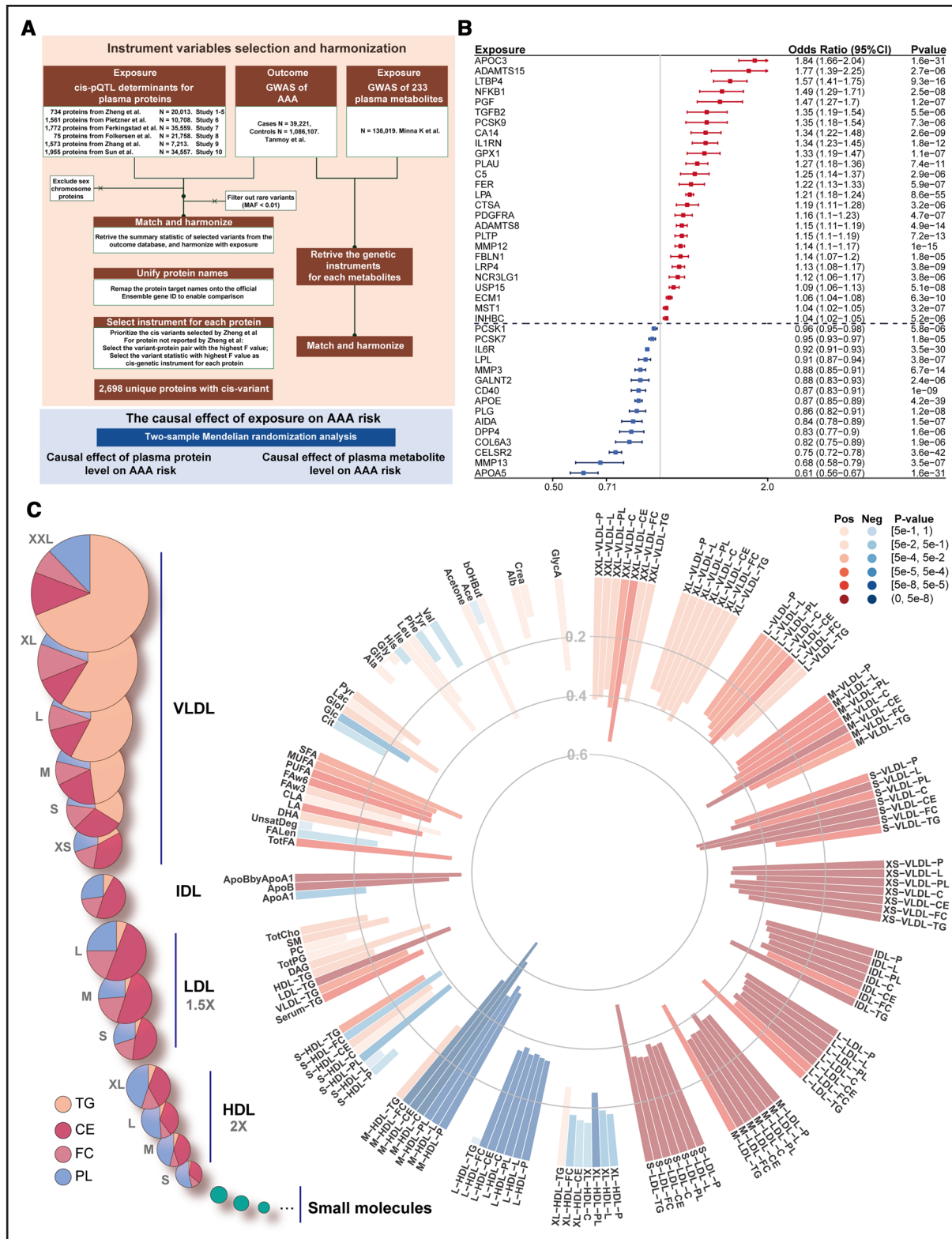


Figure 1. Mendelian randomization identifies circulating proteins and metabolites causally related to abdominal aortic aneurysm risk.

A, Outline of the analyses performed. Two-sample Mendelian randomization analyses were applied to determine the causal effects of circulating proteins, and nuclear magnetic resonance measured circulating metabolites for the risk of abdominal aortic aneurysm using multiple data sources.

B, Forest plot displaying the causal effects of 41 proteins identified through Mendelian randomization-Wald ratio analysis after Bonferroni correction. **C**, Classifications of nuclear magnetic resonance metabolites and the relative lipid compositions of the 14 lipoprotein subclasses (**D**). All 14 lipoprotein subclass particles are illustrated using the same size scale, with diameters based on mean values from 5651 (Continued)

Figure 1 Continued. participants in the Northern Finland Birth Cohort 1966. Note that the size of the low-density lipoprotein (LDL) and high-density lipoprotein (HDL) particles in the figure is multiplied by 1.5 and 2.0, respectively. The **right** side features a circular histoplot of the Mendelian randomization results for 141 metabolites. The height of each bar represents the absolute effect size, whereas the color indicates the direction and P value as determined by the Mendelian randomization inverse-variance weighted method. AAA indicates abdominal aortic aneurysm; CE, cholesterol ester; *cis*-pQTL, *cis*-acting protein quantitative trait locus; FC, free cholesterol; GWAS, genome-wide association study; IDL, intermediate-density lipoprotein; L, large; M, medium; PL, phospholipids; S, small; TG, triglyceride; VLDL, very low-density lipoprotein; XL, very large; XS, very small; and XXL, extremely large.

factors for AAA, TG was the top-ranked independent risk factor for AAA, with a marginal inclusion probability of 0.81 ($P=0.007$; Table S3). Consistent with previous studies,^{6–8} LDL-C, HDL-C, and APOA1 were still significant factors (Table S3). These genetic and proteomic findings indicate that TG-related metabolism may play a substantial role in AAA pathogenesis.

To further identify genetic associations between circulating metabolic traits and AAA risk, we used the data from a recently published GWAS study of 233 circulating metabolites to perform a 2-sample MR analysis.²⁰ The nuclear magnetic resonance–measured metabolites included 213 lipid traits (lipids, lipoproteins, and fatty acids) and 20 nonlipid traits (amino acids, ketone bodies, and glucose/glycolysis-related metabolites).²⁰ Lipoproteins are classified by particle size (extremely large, very large, large, medium, small, and very small) and then subgrouped by the components (particle number, phospholipids, cholesterol, cholesterol ester, free cholesterol, and TGs). For each metabolite, we used the inverse-variance weighted method as the primary MR approach and MR-Egger analysis and weighted median-based regression methods as sensitivity analyses. We demonstrated that TG-rich lipoproteins, including VLDL, intermediate-density lipoprotein, and LDL, and all components in TRL particles were positively associated with AAA risk, whereas HDL and glucose were negatively associated with AAA risk, consistent with population findings (Figure 1C; full MR results in Table S4).^{9,10,21,22} Interestingly, we noticed that the TG component in HDL particles was positively associated with AAA risk compared with other components in HDL particles, such as cholesterol and phospholipids (Figure 1C). Concomitantly, we observed that total fatty acids and saturated fatty acids, the major metabolites of TGs, were also positively associated with AAA risk. These findings raise the possibility that lowering TGs and related metabolites could provide a therapeutic pathway for reducing the risk of AAA.

Impaired LPL Activity Accelerates AAA Development and Rupture

Chronic subcutaneous infusion of AngII serves as a well-established AAA model in hypercholesterolemic mice, which includes using mice with deficiency in *Apoe* or *Ldlr* (LDL receptor) or manipulation by adeno-associated virus–mediated overexpression (OE) of *Pcsk9* to induce hyperlipidemia.^{23–25} Our previous GWAS demonstrated

that LPL variants that lead to increased plasma TG concentration were linked to an increased risk of AAA.⁶ The MR analysis also identified circulating LPL levels to be negatively associated with AAA risk (Figure 1B). To validate whether increased TG concentration caused by impaired LPL activity can result in AAA development and rupture, we infused AngII into male inducible *Lpl*-deficient (*iLpt*^{−/−}) mice fed a low-cholesterol Western diet. With AngII infusion, an aortic rupture occurred in 94% (16 of 17, combined data from 2 independent studies) of *iLpt*^{−/−} mice compared with 9.5% (2 of 21, combined data from 2 independent studies) in littermate control mice (Figure 2A through 2C; Figure S1). The only surviving *iLpt*^{−/−} mouse did not have AAA and had a plasma TG concentration of 474 mg/dL and a TC concentration of 233 mg/dL. In contrast, after 1 week of Western diet feeding but before AngII infusion, the majority of the *iLpt*^{−/−} mice had severely increased TG concentrations, which were as high as 11103 mg/dL (4077 ± 3218 mg/dL) compared with 66 ± 28 mg/dL in *Lpt*^{+/+} mice (Figure S1A). Saline infusion, as a control, did not cause aortic rupture in either genotype (Figure S1C). These findings showed that severely increased TG concentrations as a consequence of LPL deficiency resulted in aortic rupture and death in the AngII-induced AAA model.

Then, we employed other mouse strains with increased, but not severely elevated TG concentrations to validate our hypothesis. We performed all following AAA studies in mice fed a standard rodent laboratory diet to minimize the effects of hypercholesterolemia induced by a Western diet. ApoA-V is produced in the liver and secreted into circulation, where it exerts an important role in regulating plasma TG concentrations by enhancing LPL activity to hydrolyze TGs. Male *Apoa5*-deficient mice showed a 2- to 3-fold increase in TG concentration but no difference in TC concentration (Figure 2F and 2G; Figure S2A and S2B), consistent with previous findings.¹² Using size exclusion chromatography, we found increased TG concentrations in VLDL and intermediate-density lipoprotein (Figure S2D and S2E) in the *Apoa5*-deficient mice compared with their littermate wild-type (WT) controls, whereas cholesterol concentrations remained similar. Plasma nonesterified fatty acids (NEFAs), which are primarily released during TG hydrolysis, were also significantly elevated in the *Apoa5*-deficient mice (Figure S2C). AAA was evaluated after a 4-week AngII infusion (Figure 2D). The hypertriglyceridemic *Apoa5*-deficient mice had an increased AAA incidence and larger maximal abdomi-

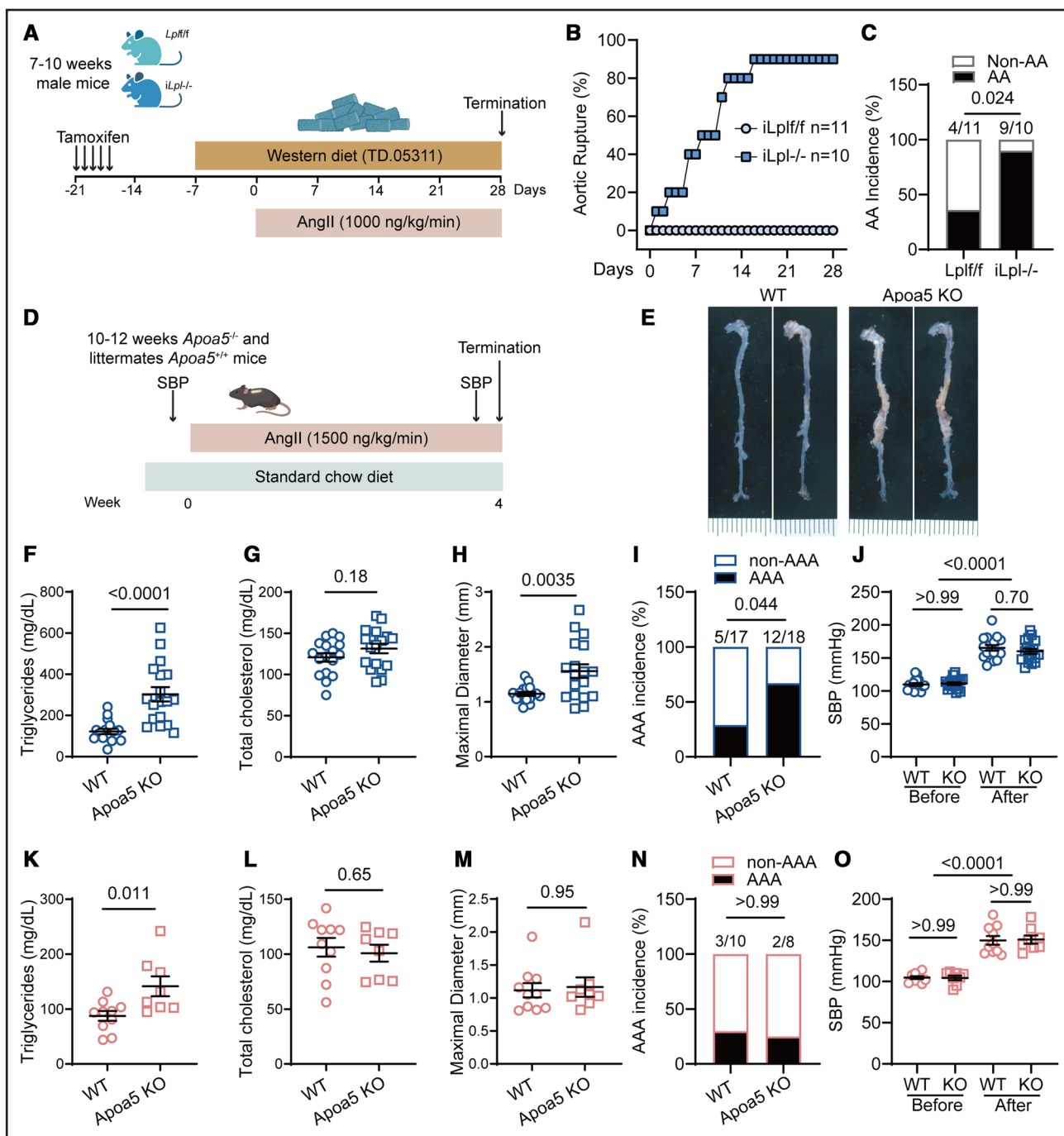


Figure 2. Impaired LPL activity accelerates abdominal aortic aneurysm development and aortic rupture.

A, Design of the abdominal aortic aneurysm (AAA) study in *Lpl*-deficient mice. Inducible global *Lpl*-deficient mice were generated by crossing *Lpl* floxed (*Lpl^{f/f}*) mice with β-actin–driven tamoxifen-inducible MerCreMer transgenic mice. Low-cholesterol, Western diet feeding was initiated 2 weeks after the start of tamoxifen treatment. **B**, Aortic rupture incidence curve during 4 weeks of angiotensin II infusion (*Lpl^{f/f}*, n=11; inducible *Lpl*-deficient, n=10). **C**, Aortic aneurysm incidence in *Lpl^{f/f}* (n=11) and inducible *Lpl*-deficient (n=10) mice. **D**, Design of the AAA study in *Apoa5*-deficient mice. Mice were fed a standard rodent laboratory diet. After 4 weeks of AngII infusion, aortas from surviving mice were harvested. **E**, Representative aortas of male wild-type (n=17) and *Apoa5*-deficient (n=18) mice after 4 weeks of AngII infusion. Plasma samples were collected on day 28 and subjected individually to analytical chemistry to measure triglycerides and total cholesterol. **F** through **J**, The triglycerides (**F**), total cholesterol (**G**), maximal aortic diameter (**H**), AAA incidence (**I**), and systolic blood pressure (**J**) in male mice. **K** through **O**, triglycerides (**K**), total cholesterol (**L**), maximal aortic diameter (**M**), AAA incidence (**N**), and systolic blood pressure (**O**) in female WT (n=10) and *Apoa5*-deficient (n=8) mice in the AngII-induced AAA study. Data are presented as circles and mean±SEM (**F** through **H**, **J** through **M**, and **O**). Statistical analyses were conducted as follows: Fisher exact test for **C**, **I**, and **N**; Student *t* test for **F**, **G**, **H**, **K**, and **L**; Mann-Whitney *U* test for **M**; and 2-way mixed-effects ANOVA followed by Sidak post hoc analysis for **J** and **O**. Scale bars=1 mm (each interval) in **E**. AngII indicates angiotensin II; *Apoa5*, apolipoprotein a5; *iLpl^{-/-}*, inducible *Lpl*-deficient; KO, knock out; SBP, systolic blood pressure; and WT, wild-type.

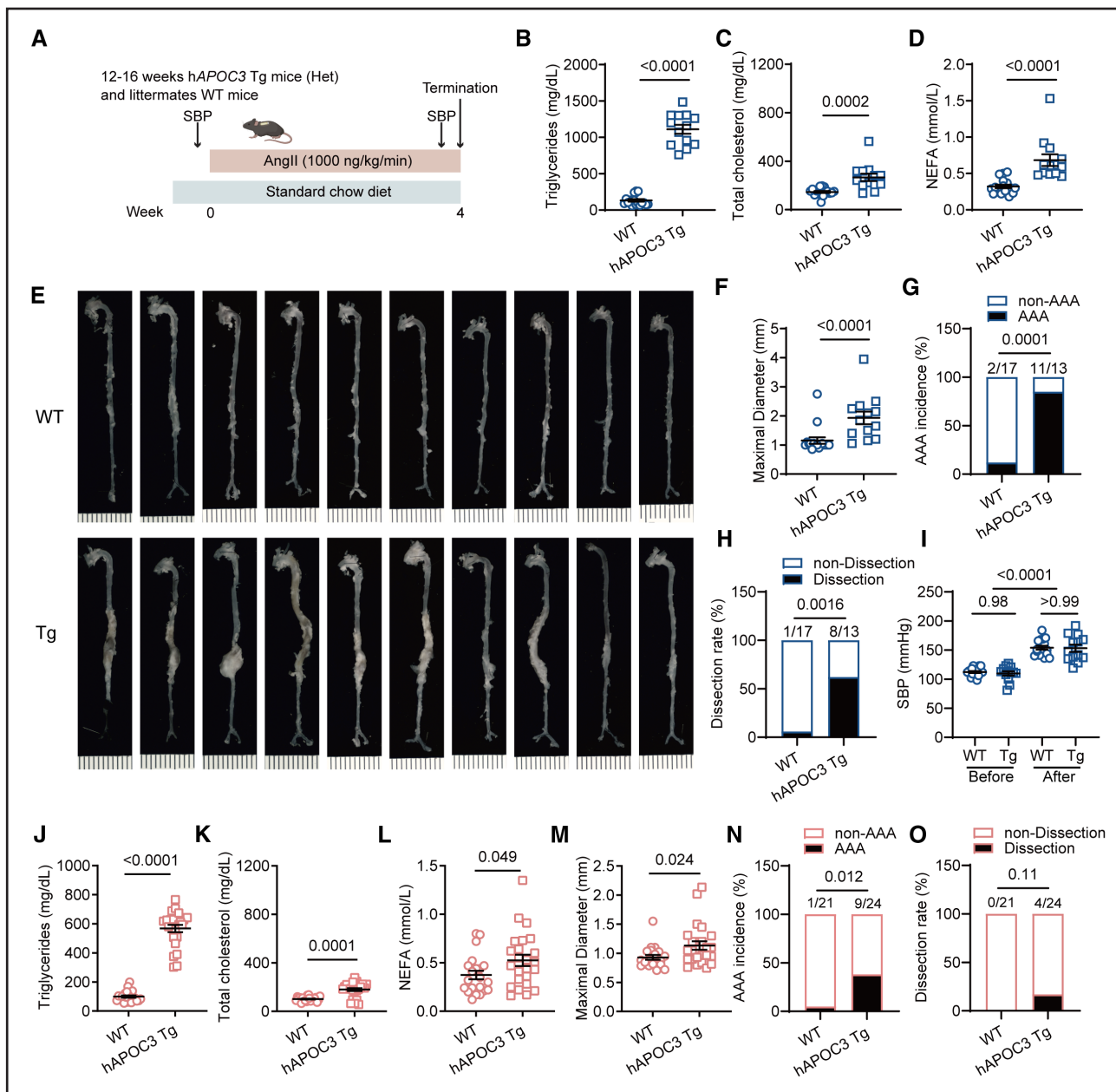


Figure 3. Dramatically increased triglyceride concentrations accelerate abdominal aortic aneurysm development and dissection in human APOC3 transgenic mice.

A, Design of the abdominal aortic aneurysm study in human APOC3 transgenic mice. Twelve- to 16-week-old human APOC3 transgenic mice (n of males=15; n of females=24) or wild-type (WT) littermates (n of males=17, n of females=21) were infused with angiotensin II (1000 ng/kg/min) for 4 weeks to induce an abdominal aortic aneurysm. Systolic blood pressure was measured before and after angiotensin II infusion. The mice were fed a standard rodent laboratory diet. After 4 weeks, aortas from surviving mice were harvested. Plasma samples were collected on day 28 and subjected individually to analytical chemistry. **B** through **D**, plasma triglycerides (**B**), total cholesterol (**C**), and nonesterified fatty acids (**D**) in male mice. **E**, Representative aortas of male wild-type and human APOC3 transgenic mice after 4 weeks of angiotensin II infusion. **F** through **I**, Maximal aortic diameter (**F**), abdominal aortic aneurysm incidence (**G**), dissection rate (**H**), and systolic blood pressure (**I**) in male mice. **J** through **O**, The triglycerides (**J**), total cholesterol (**K**), nonesterified fatty acids (**L**), maximal aortic diameter (**M**), abdominal aortic aneurysm incidence (**N**), and dissection rate (**O**) in female WT and human APOC3 transgenic mice after 4 weeks of angiotensin II infusion. Data are presented as circles and mean \pm SEM. Statistical analyses were conducted as follows: Mann-Whitney *U* test for **B**, **D**, **F**, **J**, and **K**; Student *t* test for **C**, **L**, and **M**; Fisher exact test for **G**, **H**, **N**, and **O**; and 2-way mixed-effects ANOVA followed by Sidak post hoc analysis for **I**. Scale bars=1 mm (each interval) in **E**. AngII indicates angiotensin II; hAPOC3 Tg, human APOC3 transgenic; NEFA, nonesterified fatty acid; SBP, systolic blood pressure; and WT, wild-type.

nal aorta diameter (Figure 2E, 2H, and 2I). Slightly increased TG concentrations in *Apoa5*-deficient mice promoted AAA formation but did not trigger aneurysm rupture and animal death (Figure S11). There was no difference in blood pressure before and after AngII infusion between *Apoa5*-deficient mice and their littermate controls (Figure 2J). This phenotype was not observed in *Apoa5*-deficient female mice (Figure 2K through 2O), which had significantly lower TG concentrations compared with male *Apoa5*-deficient mice (142 ± 51 mg/dL versus 303 ± 146 mg/dL, $P=0.006$; Figure 2F and 2K). In addition, female mice demonstrate a markedly lower incidence of AAA than male mice, consistent with the well-documented male sex predominance reported in the literature.²⁶ These findings imply a causative role of elevated TG concentrations in AAA pathogenesis.

Dramatically Increased TG Levels Accelerate AAA Development and Dissection in Human APOC3 Transgenic Mice

Increased plasma ApoC-III concentrations are linked to enhanced production and slowed clearance of TG-rich lipoproteins, causing hypertriglyceridemia. Human *APOC3* transgenic (h*APOC3* Tg) mice and age/sex-matched WT littermates were fed a standard rodent laboratory diet (Figure 3A). Compared with controls, male h*APOC3* Tg mice had an about 8-fold increase in plasma TG concentrations (Figure 3B) and an about 1-fold elevation in plasma TC concentrations (Fig 3C) and NEFAs (Figure 3D). We observed a low incidence of AAA in WT littermates (2 of 17), similar to the literature.²⁶ However, there was a dramatically increased AAA incidence and a larger maximal diameter of the suprarenal aorta in h*APOC3* Tg mice (11 of 13 surviving animals) as well as a higher dissection rate (8 of 13 surviving animals), and another 2 mice died from AAA rupture (Figure 3E through 3H; Figure S11). There was no difference in systolic blood pressure between h*APOC3* Tg mice and controls (Figure 3I). A similar phenotype was observed in female mice (Figure 3J through 3O), which had a 5-fold increase in TG concentrations compared with control mice, indicating that dramatically increased TG concentrations accelerated AAA development, surpassing the protective effects of female hormones.

The effects of increased TG concentrations on AAA development were also evaluated in a PPE (porcine pancreatic elastase)-induced AAA model, in which AAA progression is independent of hypercholesterolemia.²⁷ Based upon a 50% increase in the maximal abdominal aorta diameter as AAA on postoperative day 14, the incidence of AAA was 100% for both male and female h*APOC3* Tg and littermate control mice (Figures S3 and S4). Male h*APOC3* Tg mice showed significantly larger maximal aortic diameters than littermate controls, dem-

onstrating that increased TG concentrations accelerated AAA growth (Figure S3A through S3E). Even though female h*APOC3* Tg mice had lower TG concentrations than male mice (635 ± 36 mg/dL versus 946 ± 258 mg/dL, $P=0.0005$), the increased TG concentrations in female mice were sufficient to cause larger aortic diameters (Figure S4A through S4D).

These findings from the 3 hypertriglyceridemia mouse models indicate that increased TG concentrations accelerate AAA rupture and aneurysm growth.

Palmitate and Increased TG Concentrations Inhibit Lysyl Oxidase Maturation in Human Aortic Smooth Muscle Cells and Aortas

The pathophysiology of AAA is intricately linked to the disruption of smooth muscle cell homeostasis within the aortic wall, including phenotypic switching, cell death, extracellular matrix (ECM) remodeling, and inflammatory responses.²⁸ Serum from *Apoa5*-deficient or h*APOC3* Tg mice, as well as VLDL and HDL particles, did not affect primary human aortic smooth muscle cell (HASMC) viability (Figure S5). OE of APOC3 in h*APOC3* Tg mice caused elevated plasma TG concentrations accompanied by increased plasma NEFA concentrations (Figure 3D; Figure S3C). The high availability of fatty acids in the liver further increases TG synthesis, resulting in VLDL assembly and secretion. Using MR, we confirmed the causal association between genetically determined plasma TG level and circulating total fatty acid concentrations (Fig 4A). Palmitic acid (PA; 16:0), stearic acid (18:0), palmitoleic acid (16:1n-7), and oleic acid (18:1n-9) are major saturated and monounsaturated fatty acids that affect cellular signaling and metabolic pathways.²⁹ PA is the most common saturated fatty acid in the human body, typically accounting for 20% to 30% of the total fatty acids.³⁰ MR analysis found that increased TGs causally increased the PA level but not the other 3 fatty acids (Figure 4A), suggesting that PA serves as an important metabolite in mediating the AAA-promoting effects of high TG or high TG-related mutations. Using untargeted metabolomics, we found elevated plasma ethyl palmitate levels (a lipid-soluble form of PA) in h*APOC3* Tg mice (Figure 4B). Bulk RNA-seq analysis was performed to compare PA-incubated HASMCs with BSA-treated (vehicle control) cells. Compared with the BSA-incubated group, PA-incubated HASMCs showed an apparent reduction in ECM assembly pathways, including collagen chain trimerization, elastic fiber formation and maturation (Figure 4C through 4E), and increased expression of inflammation-related genes (Figure S6A and S6B; Table S5).

Transforming growth factor β and lysyl oxidase (LOX) are crucial in regulating the cross-linking of collagen and elastin in the ECM. LOX was unexpectedly upregulated

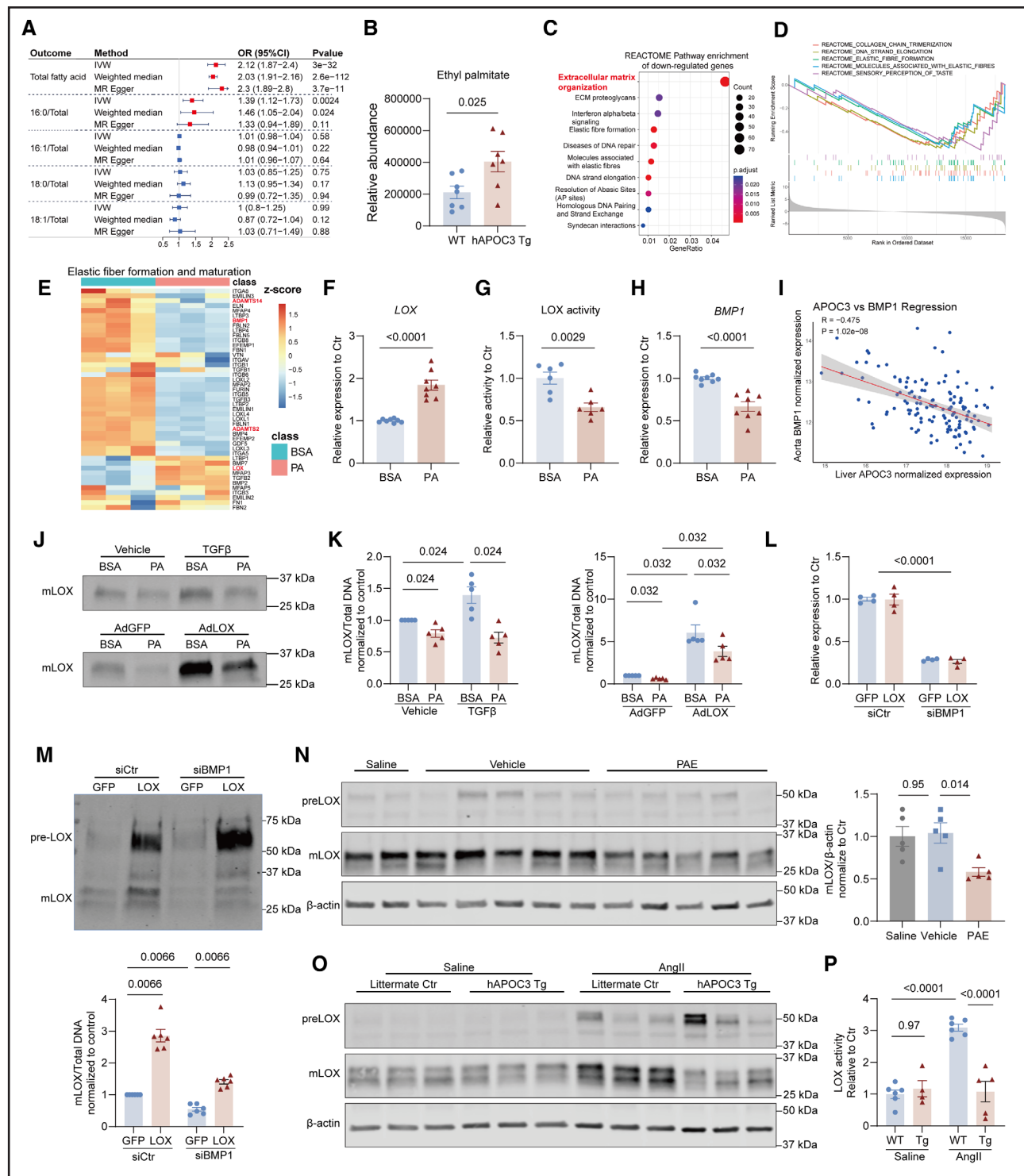


Figure 4. Palmitic acid inhibits lysyl oxidase maturation in human aortic smooth muscle cells and aortas.

A, Two-sample mendelian randomization to detect the causal effects of triglycerides on circulating total fatty acid, palmitic acid (PA; 16:0), stearic acid (18:0), palmitoleic acid (16:1n-7), and oleic acid (18:1n-9) levels. **B**, Untargeted metabolomics was applied to measure the ethyl palmitate levels in plasma from 14 to 18-week-old male human *APOC3* transgenic (heterozygous) mice ($n=7$) and littermate controls ($n=7$). **C** through **H**, Human aortic smooth muscle cells were starved in OptiMEM-reduced serum medium for 24 hours, followed by incubation with PA (250 μ M) or vehicle (BSA) for another 24 hours. Total RNA was extracted for RNA sequencing ($n=3$ /group) or qPCR. **C**, Reactome pathway enrichment analysis of downregulated genes in the PA group. Dot size represents the number of downregulated genes associated with each Reactome pathway. Dot color indicates the statistical significance, shown as the Benjamini-Hochberg-adjusted P value derived from over-representation analysis using the hypergeometric test. The gene ratio is defined as the number of downregulated genes annotated to a given pathway divided by the total number of downregulated genes analyzed. **D**, Top 5 downregulated Reactome pathways identified from gene set enrichment (Continued)

Figure 4 Continued. analysis. The gene set enrichment analysis enrichment plot shows whether a gene set (pathway) is concentrated at the top or bottom of a ranked gene list. Each line represents the running enrichment score, with a peak on the **right** indicating enrichment in downregulated genes. Vertical bars mark the positions of the gene set within the ranked list. The **bottom** displays the ranking metric (\log_2 fold change). **E**, Heatmap of gene expression levels involved in elastic fiber formation and maturation. Color represents the Z score of the expression of each gene, with red indicating higher and blue indicating lower expression relative to the mean of the gene across samples. **F** and **H**, qPCR analysis of *LOX* (lysyl oxidase) (**F**) and *BMP1* (**H**) ($n=8$ /group, data from 4 independent experiments). **G**, LOX activity in the conditioned medium ($n=6$ /group, data from 2 independent experiments). Cell total DNA was used for normalization. **I**, Correlation between liver *APOC3* expression level and aortic *BMP1* expression level among 131 donors in the GTEx project. Correlation coefficient was calculated using Pearson's method. The fitted lines represent the linear regression, with shaded bands indicating the 95% CI. **J** and **K**, Human aortic smooth muscle cells were starved in OptiMEM for 24 hours and then incubated with PA (250 μ M) or vehicle along with transforming growth factor β (10 ng/mL) or vehicle for another 24 hours, or human aortic smooth muscle cells were transfected with adenovirus GFP (green fluorescent protein) or LOX (30 multiplicity of infection) for 6 hours in a growth medium and then starved in OptiMEM for another 24 hours. Cells were incubated with PA (250 μ M) or vehicle for an additional 24 hours. Conditioned medium was collected for Western blot analysis. Cell total DNA was used for normalization. **J**, Representative Western blot image of mature LOX in conditioned medium ($n=5$ /group). **K**, Quantification analysis of mature LOX protein abundance ($n=5$ /group). **L** and **M**, Human aortic smooth muscle cells were transfected with siBMP1 at 1 nM or siCtr with RNAimax for 6 hours in OptiMEM-reduced serum medium and then transfected with adenovirus GFP or LOX (30 multiplicity of infection) for another 23 hours in OptiMEM-reduced serum medium. The conditioned medium was used for Western blot analysis, and whole cells were used for RNA extraction or DNA extraction. **L**, qPCR analysis of *BMP1* ($n=4$ /group). **M**, Representative LOX expression in conditioned medium (**top**) and quantification analysis (**bottom**, $n=6$ /group). **N**, Eight-week-old male C57BL/6J mice were given saline, vehicle, or ethyl palmitate (600 mg/kg) for 5 consecutive days via intraperitoneal injection. On day 6, mice were euthanized, suprarenal abdominal aortas were isolated, and total protein was extracted and analyzed by Western blot to detect LOX abundance in suprarenal abdominal aortas, with corresponding quantifications for mature LOX ($n=5$ /group). **O**, Twelve- to 16-week-old human *APOC3* transgenic mice and littermate control mice were infused with saline or angiotensin II (1000 ng/kg/min) for 7 days. On day 8, mice were euthanized, suprarenal abdominal aortas were isolated, and total protein was extracted and analyzed by Western blot to detect LOX expression in suprarenal abdominal aortas, with corresponding quantifications for mature LOX ($n=3$ or 4/genotyping/treatment). **P**, Fourteen- to 20-week-old human *APOC3* transgenic mice and littermate control mice were infused with saline or angiotensin II (1000 ng/kg/min) for 7 days. On day 8, mice were euthanized, suprarenal abdominal aortas were isolated, and LOX activity was measured ($n=4$ –6/genotyping/treatment). Data are presented as dots and mean \pm SEM (**B**, **F** through **H**, and **K** through **P**). Statistical analyses were conducted as follows: Student *t* test for **B** and **F** through **H**, Mann-Whitney *U* test followed by Bonferroni correction for **K** and **M**, 2-way ANOVA followed by Sidak post hoc analysis for **L** and **P**, and 1-way ANOVA followed by Sidak post hoc analysis for **N**. ECM indicates extracellular matrix; GTEx, Genotype-Tissue Expression; h*APOC3* Tg, human *APOC3* transgenic; IVW, inverse-variance weighted; MR, Mendelian randomization; OR, odds ratio; PAE, ethyl palmitate; qPCR, quantitative real-time polymerase chain reaction; and WT, wild-type.

compared with the most downregulated genes in the elastic fiber formation and maturation pathways (Figure 4E). In primary HASMCs, PA incubation induced the transcription of LOX, showing increased mRNA abundance by quantitative real-time polymerase chain reaction (Figure 4F). However, PA treatment paradoxically decreased LOX activity in the conditioned medium of HASMCs (Figure 4G), indicating that PA may impair LOX protein maturation or posttranslational modification. LOX is initially synthesized as a preproprotein, which undergoes several posttranslational modifications for its maturation and functional activation. Impairments in LOX activity, whether because of genetic mutations or LOX inhibitors, can lead to AAA formation and rupture.^{31–33} Our RNA-seq data indicated that PA incubation downregulated the expression of BMP-1 (bone morphogenetic protein 1), ADAMTS2 (a disintegrin and metalloproteinase with thrombospondin motif 2), and ADAMTS14, which are critical enzymes controlling LOX activation by the proteolytic removal of the propeptide region.³⁴ We further confirmed that PA incubation downregulated BMP-1 and ADAMTS2 transcription in HASMCs (Figure 4H; Figure S7A). Immunoblot analyses demonstrated that incubation with transforming growth factor β increased the abundance of the mature form of LOX both in the conditioned medium and cell lysates of HASMCs. However, the presence of PA blocked its effect, resulting in a less mature LOX (Figure 4J and 4K; Figure S7H). LOX OE

increased the mature form of LOX in HASMCs, which was suppressed by incubation with PA (Figure 4J and 4K; Figure S7I), indicating that PA interferes with the maturation process of LOX in HASMCs.

To investigate how PA influences LOX maturation, using small interfering RNA-mediated gene silencing of *BMP1*, *ADAMTS2*, or *ADAMTS14* in HASMCs, we found that *BMP1* knockdown led to dramatically decreased LOX maturation in the conditioned medium (Figure S7E and S7F), suggesting that BMP-1 is the primary enzyme regulating LOX maturation in HASMCs. Additionally, *BMP1* knockdown increased LOX transcription (Figure S7G), likely as a compensatory effect; however, it was insufficient to compensate for the loss of mature LOX. Next, we investigated whether LOX OE can restore mature LOX levels within the PA-BMP-1 axis. In the presence of PA or knockdown of *BMP1*, LOX maturation was largely impaired (Figure 4J, 4K, and 4M), showing dramatically reduced mature bands. OE of LOX restored mature LOX levels (Figure 4J, 4K, and 4M), suggesting that LOX OE may prevent the pro-AAA effects of high TG and PA levels. Our previous study validated the use of tissue-crosstalk analysis for investigating organ-organ interactions.³⁵ Among the >1800 secreted proteins in the liver, *APOC3* ranked 52nd in terms of its impact on aortic gene expression. Among the 131 donors from the Genotype-Tissue Expression project, liver *APOC3* RNA expression showed a strong negative association with

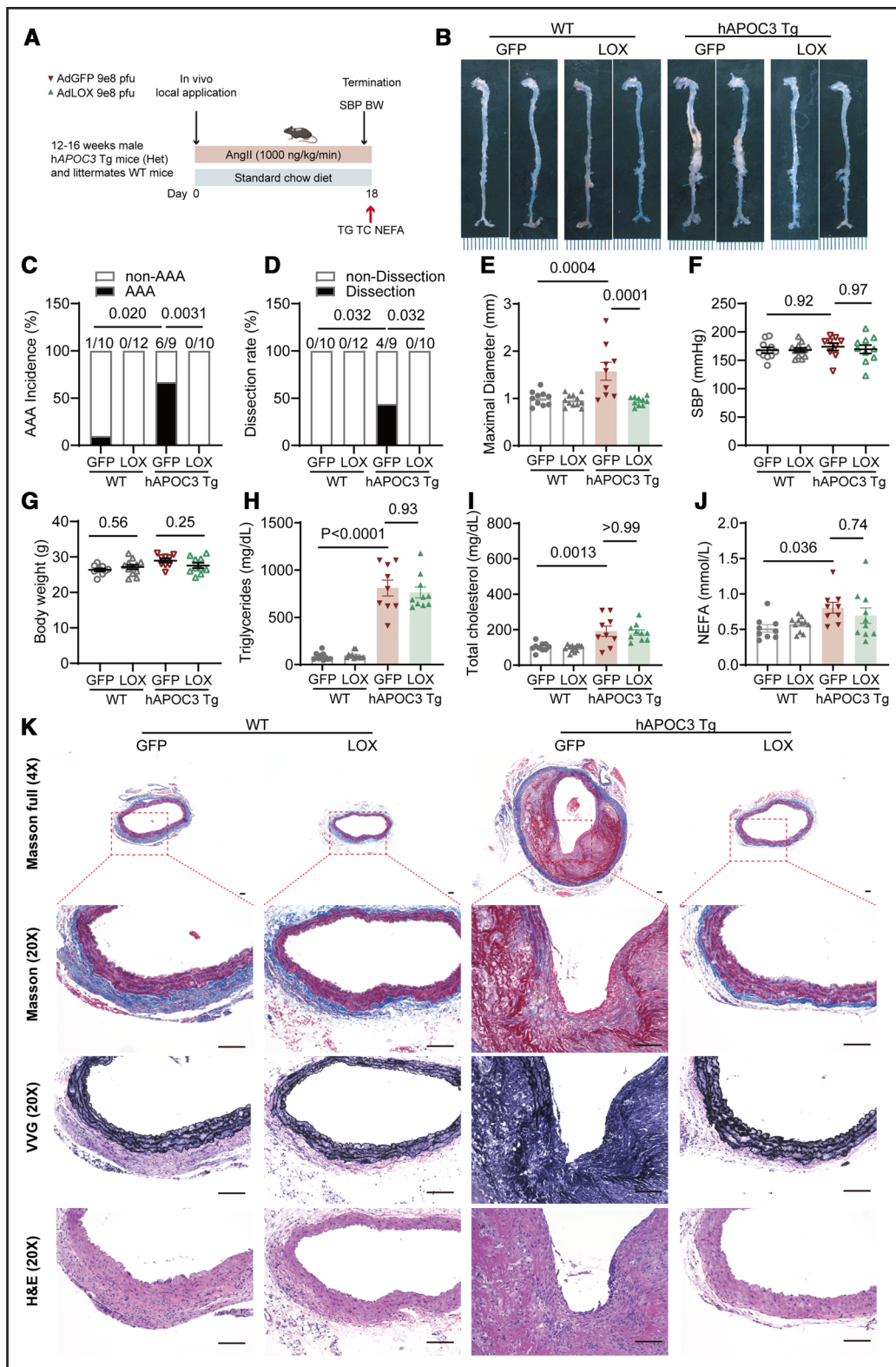


Figure 5. Lysyl oxidase overexpression inhibits abdominal aortic aneurysm formation and dissection in human APOC3 transgenic mice.

A, Design of the lysyl oxidase (LOX) overexpression study in human APOC3 transgenic mice. Twelve- to 16-week-old male human APOC3 transgenic mice and their littermate wild-type controls were transfected with 9×10^8 plaque-forming unit adenovirus GFP (green fluorescent protein) or LOX to the suprarenal abdominal aorta and then infused with angiotensin II (1000 ng/kg/min) for 18 days to induce an abdominal aortic aneurysm. The surviving mice were used for the following analysis (wild-type, GFP: n=10; wild-type, LOX: n=12; transgenic, GFP, n=9; transgenic, LOX, n=10). **B**, Representative aortic trees from the 4 groups. **C** through **E**, Quantification of abdominal aortic aneurysm (Continued)

Figure 5 Continued. incidence (**C**), dissection rate (**D**), and maximal aorta diameter (**E**) among the 4 groups. **F** through **J**, Systolic blood pressure (**F**), body weight (**G**), plasma triglycerides (**H**), total cholesterol (**I**), and nonesterified fatty acids (**J**). **K**, Representative Masson trichrome, Verhoeff-van Gieson, and H&E staining of suprarenal abdominal aorta sections. Data are presented as dots and mean \pm SEM (**E** through **J**). Statistical analyses were conducted as follows: Fisher exact test for **C** and **D**, 2-way ANOVA followed by Sidak post hoc analysis for **E** through **J**. Scale bars=1 mm (each interval) in **B** and 100 μ m in **K**. AngII indicates angiotensin II; BW, body weight; hAPOC3 Tg, human APOC3 transgenic; NEFA, nonesterified fatty acid; SBP, systolic blood pressure; TC, total cholesterol; TG, triglyceride; VVG, Verhoeff-van Gieson; and WT, wild-type.

BMP1 RNA expression in the aorta (Figure 4I), whereas the associations with *ADAMTS2* and *ADAMTS14* were much weaker (Figure S7B and S7C). In contrast, liver *APOC3* expression was positively associated with aortic LOX expression (Figure S7D). The tissue crosstalk analysis suggests that liver-secreted APOC3 regulates aortic gene expression, including *BMP1* and LOX, essential for vascular integrity, potentially influencing aortic ECM remodeling and contributing to AAA pathogenesis.

To investigate the effects of increased circulating palmitate concentrations on the maturation of LOX in aortas, we administered ethyl palmitate, which can be hydrolyzed to free palmitate in rodents.³⁶ The mature LOX abundance in suprarenal abdominal aortas was decreased significantly after administration of ethyl palmitate compared with the vehicle or saline control aortas (Figure 4N). Then, we examined whether increased TG concentrations affected the maturation and activity of LOX in the aortas of hAPOC3 Tg and littermate control mice. There was no difference in the abundance of mature LOX and LOX activity in suprarenal abdominal aortas between the 2 groups without AngII infusion (Figure 4O and 4P; Figure S7J). We observed a dramatic upregulation of mature LOX and LOX activity upon AngII infusion in control mice (Figure 4O and 4P; Figure S7J), suggesting a protective and compensatory mechanism to enhance elastic fiber assembly to protect against the effects of AngII. However, this response was absent in hAPOC3 Tg mice (Figure 4O and 4P; Figure S7J), indicating that increased TG or palmitate inhibited LOX maturation and LOX activity in the aortas, which may contribute to AAA development and rupture.

LOX OE Effectively Prevents AAA Formation and Dissection in hAPOC3 Tg Mice

These findings suggest that TG and palmitate promote AAA development by disrupting essential LOX maturation. To validate this mechanism in vivo, we used an adenoviral vector to overexpress LOX in the suprarenal abdominal aorta of both WT and hAPOC3 Tg mice, followed by an 18-day AngII infusion (Figure 5A). First, we confirmed that local adenovirus application successfully increased the expression of LOX or GFP (green fluorescent protein; as control) in the target region (Figure S8). LOX OE did not affect the rupture rate (Figure S11) or induce AAA formation in WT mice (Figure 5B through 5E). Strikingly, none of the hAPOC3 Tg mice

developed AAA when LOX was overexpressed locally alongside AngII induction compared with a 67% AAA incidence and a 44% dissection rate in the GFP-overexpressing control group (Figure 5B through 5D). LOX OE significantly reduced the maximal suprarenal abdominal aorta diameter (Figure 5E) without affecting systolic blood pressure (Figure 5F), body weight (Figure 5G), TG (Figure 5H), TC (Figure 5I), and NEFA levels (Figure 5J). Histological analysis revealed that hAPOC3 Tg mice exhibited substantial collagen disorganization and elastic fiber degradation compared with WT mice, indicating impaired LOX function (Figure 5K). Notably, LOX OE restored these structural features and reinforced vascular wall integrity even in the presence of elevated TG levels (Figure 5K). Taken together, these results established that impaired LOX activation is a key mechanism by which elevated TG levels contribute to AAA development.

Angptl3 antisense oligonucleotide Inhibits AAA Formation and Dissection in hAPOC3 Tg Mice

Based on the above findings, we asked whether lowering TG levels could attenuate AAA formation and dissection. We administrated fenofibrate and niacin, commonly used for treating hypertriglyceridemia, but only observed a 14% to 17% reduction of plasma TG concentration in hAPOC3 Tg mice (Figure S9). N-acetylgalactosamine-conjugated antisense nucleotide (ASO) targeting of hepatocyte ANGPTL3 results in significantly decreased plasma TG concentrations in animals and humans.^{15,16,37} In hAPOC3 Tg mice, administration of the *Angptl3* ASO dramatically suppressed hepatic *Angptl3* mRNA abundance by 64% and the plasma ANGPTL3 concentrations by 81% (Figure 6A through 6C). Consequently, administration of the *Angptl3* ASO significantly reduced concentrations of NEFA, TGs (from 1119 ± 98 mg/dL to 586 ± 114 mg/dL), and TC (from 283 ± 103 mg/dL to 117 ± 58 mg/dL) (Figure 6D through 6F). Consistent with these findings, increased TG concentrations in hAPOC3 Tg mice accelerated AAA development during AngII infusion (Figure 6G through 6L). After administration of *Angptl3* ASO to hAPOC3 Tg mice, we recorded significant reductions in AAA incidence, maximal aortic diameter, elastin degradation, and dissection, comparable with the control mice (Figure 6G through 6L). Quantitative real-time polymerase chain reaction and ELISA analyses showed no significant changes in the levels of mouse *Apoc3* and human *APOC3* (Figure 6M through

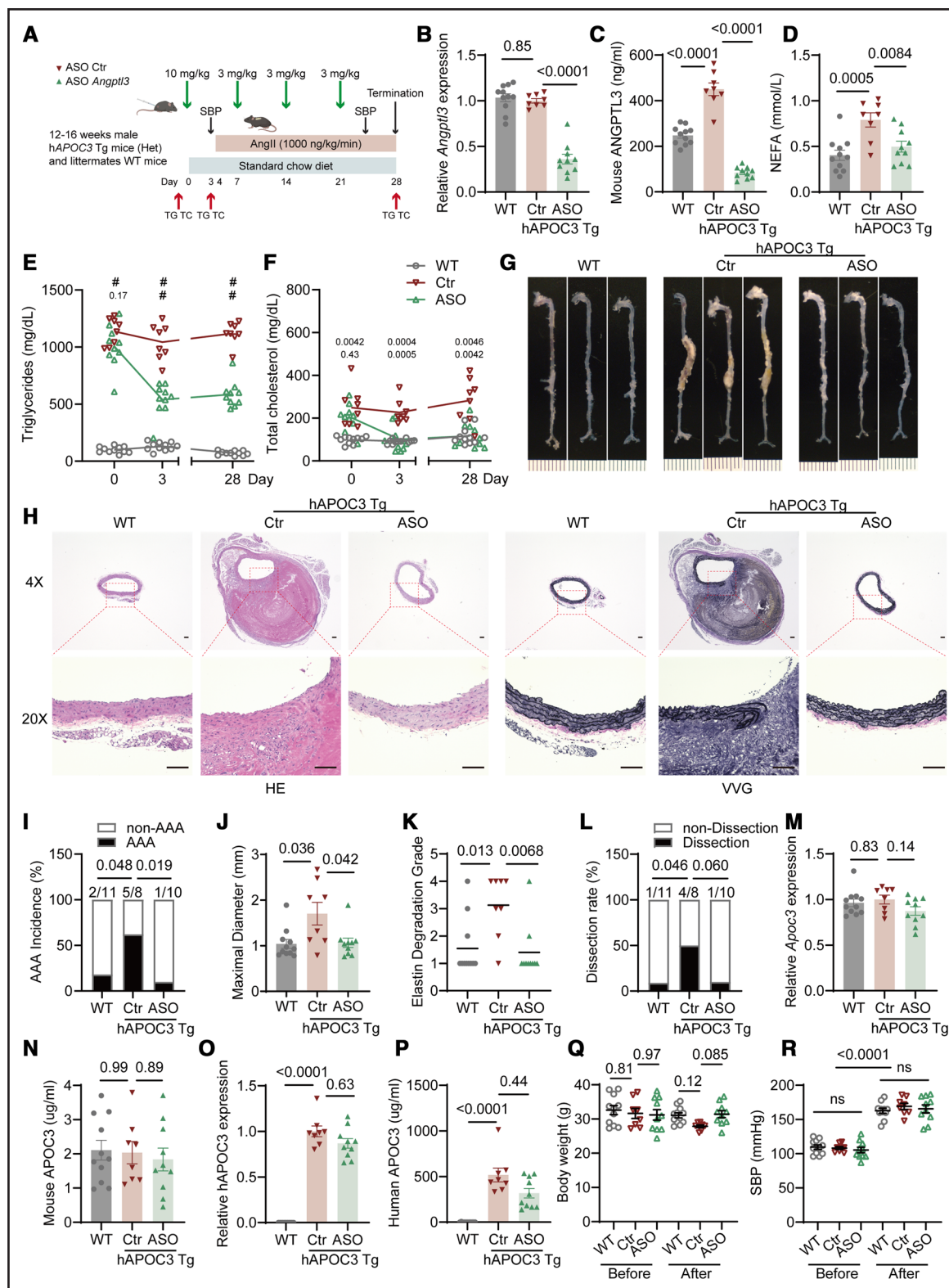


Figure 6. Administration of *Angptl3* antisense oligonucleotide prevents abdominal aortic aneurysm formation in human APOC3 transgenic mice.

A, Design of *Angptl3* antisense oligonucleotide (ASO) study in human APOC3 transgenic (Tg) mice. Twelve- to 16-week-old male human APOC3 Tg mice were given one injection of the *Angptl3* ASO (10 mg/kg) or scrambled ASO by subcutaneous administration. After 3 days, mice were infused with angiotensin II (1000 ng/kg/min) for 25 days. Three more injections (3 mg/kg) were conducted on days 7, 14, and 21. A wild-type group was included, receiving injections of scrambled ASO. At the end of the study, aortas, livers, and plasma were harvested (wild-type, n=11; Tg, ASO Ctr, n=8; Tg, ASO *Angptl3*, n=10). **B**, Relative abundance of *Angptl3* mRNA in livers of the 3 groups. **C** and **D**, Plasma ANGPTL3 protein concentrations (**C**) and nonesterified fatty acids (**D**) at the end point. **E** and **F**, Plasma triglycerides (**E**) and total (Continued)

Figure 6 Continued. cholesterol (**F**) concentrations on days 0, 3, and 28. Shown are the *P* value of the comparison between WT and Tg, ASO Ctr mice (**top**) and the comparison between Tg, ASO Ctr and Tg, ASO *Angptl3* mice (**bottom**). **G**, Representative aortic trees from the 3 groups. **H**, Representative H&E staining (**left**) and Verhoeff-van Gieson staining (**right**) of suprarenal abdominal aorta sections. **I** through **L**, Quantification of abdominal aortic aneurysm incidence (**I**), maximal aorta diameter (**J**), elastic fiber degradation score (**K**), and dissection rate (**L**) among the 3 groups. **M**, Relative abundance of *Apoc3* in the liver. **N**, Plasma mouse-specific APOC3 concentrations were measured by ELISA at the end point. **O**, Relative liver abundance of human *APOC3*. **P**, Plasma human APOC3 concentrations were determined by ELISA at the end point. **Q**, Body weight comparisons among the 3 groups before and at the end of the study. **R**, Systolic blood pressure comparisons among the 3 groups before and at the end of the study. Data are presented as circles/dots and mean \pm SEM or mean only. Statistical analyses were conducted as follows: 1-way ANOVA followed by Sidak post hoc analysis for **B**, **C**, **D**, **M**, and **N**; Kruskal-Wallis test followed by Dunn's post hoc analysis for **J**, **K**, **O**, and **P**; Fisher exact test for **I** and **L**; and 2-way mixed-effects ANOVA followed by Sidak post hoc analysis for **E**, **F**, **Q**, and **R**. Scale bars=1 mm (each interval) in **G** and 100 μ m in **H**. #*P*<0.0001. AAA indicates abdominal aortic aneurysm; AngII, angiotensin II; Ctr, control; hAPOC3 Tg, human *APOC3* transgenic; NEFA, non-esterified fatty acid; SBP, systolic blood pressure; VVG, Verhoeff-van Gieson; and WT, wild-type.

6P). There were no significant changes in the TG and TC metabolism-related genes in the liver, such as *Apoc2*, *Apoe*, *Apob*, *Mtp*, *Fasn*, *Srebp1c*, *Ldlr*, *Lrp1*, and *Pcsk9* (Figure S10). *Angptl3* ASO administration did not significantly change body weight or systolic blood pressure (Figure 6Q and 6R). Overall, our findings demonstrate that administration of the *Angptl3* ASO protected against hypertriglyceridemia-accelerated AAA development in hAPOC3 Tg mice.

Angptl3 ASO Inhibits AAA Development in Apoe-Deficient Mice

ApoE-deficient mice have high levels of VLDL because of impaired clearance of chylomicron and VLDL. Compared with age- and sex-matched C57BL/6J mice, *Apoe*-deficient mice show significantly increased plasma levels of TC and moderately increased TG levels when fed a standard rodent diet.³⁸ Similar to the observation in hAPOC3 Tg mice, administration of the *Angptl3* ASO dramatically reduced hepatic *Angptl3* mRNA expression and the circulating levels of ANGPTL3 (Figure 7A through 7C). As expected, administration of the *Angptl3* ASO significantly decreased TG concentrations by 50% and NEFA by 31% and slightly decreased TC concentrations by 8% (not significant) in *Apoe*-deficient mice fed a standard rodent laboratory diet (Figure 7D through 7F). We also used size exclusion chromatography to separate lipoprotein classes and found decreased TG concentrations, mainly in VLDL and intermediate-density lipoprotein (Figure 7I), whereas cholesterol concentrations were slightly reduced in VLDL and HDL (Figure 7J). Blood pressure measurements and body weight recordings revealed no significant difference between mice administered the control ASO and *Angptl3* ASO (Figure 7G and 7H). Consistent with the literature, AAA incidence in *Apoe*-deficient mice was 83% in the control group (Figure 7K and 7L). *Angptl3* ASO administration largely inhibited AAA development, as evidenced by significantly decreased AAA incidence and maximal aortic diameters (Figure 7L and 7M). Knockdown of hepatic *Angptl3* had limited effects on the expression of genes involved in lipogenesis and cholesterol metabolism (Figure 7N). Taken together, these data demonstrated

that lowering TG and NEFA concentrations by *Angptl3* ASO inhibited AAA development in *Apoe*-deficient mice.

DISCUSSION

AAA screening programs have identified many asymptomatic AAAs and effectively reduced aneurysm-related mortality. Thus, limiting aneurysm growth and reducing the risk of aneurysm rupture has become a key priority for the treatment of AAA.³⁹ Based on the genetic, proteomic, and metabolomic findings, using 3 hypertriglyceridemic mouse models, we identify that increased TG concentrations accelerate AAA formation, dissection, and rupture. Of clinical relevance, we provide evidence that lowering TG and NEFA concentrations by *Angptl3* ASO administration dramatically inhibited AAA development and dissection.

MR using protein quantitative trait loci as instrumental variables can help infer causality and identify drug targets for complex diseases. By integrating protein quantitative trait loci from 10 large GWASs on circulating proteins, we updated the “actionable” druggable target pool into an enlarged set of 2698 proteins. Genetically determined APOA5 and LPL, two critical molecules regulating TG metabolism, were negatively associated with AAA risk. In contrast, the variants related to APOC3 with increased TG concentrations were associated with increased AAA risk, underscoring the role of TG metabolism in human AAA development, consistent with other genetic findings.^{7,8} We further explored the causal effects of metabolites on AAA risk using instrumental variables from 233 nuclear magnetic resonance-measured circulating metabolites.²⁰ The strong associations found in VLDL and its subfractions as well as free fatty acid concentrations further highlighted the importance of TG metabolism in AAA. Collectively, these findings emphasize the significance of TG in AAA risk and provide potential candidates for AAA prevention and treatment.

According to the literature and our experience, young C57BL/6J mice, when fed a standard rodent laboratory diet, have low AAA incidence when infused with AngII.^{26,40} Hyperlipidemia increases the AAA incidence during AngII infusion in *Ldlr*- and *Apoe*-deficient mice or C57BL/6J mice with an AAV expressing a gain-of-

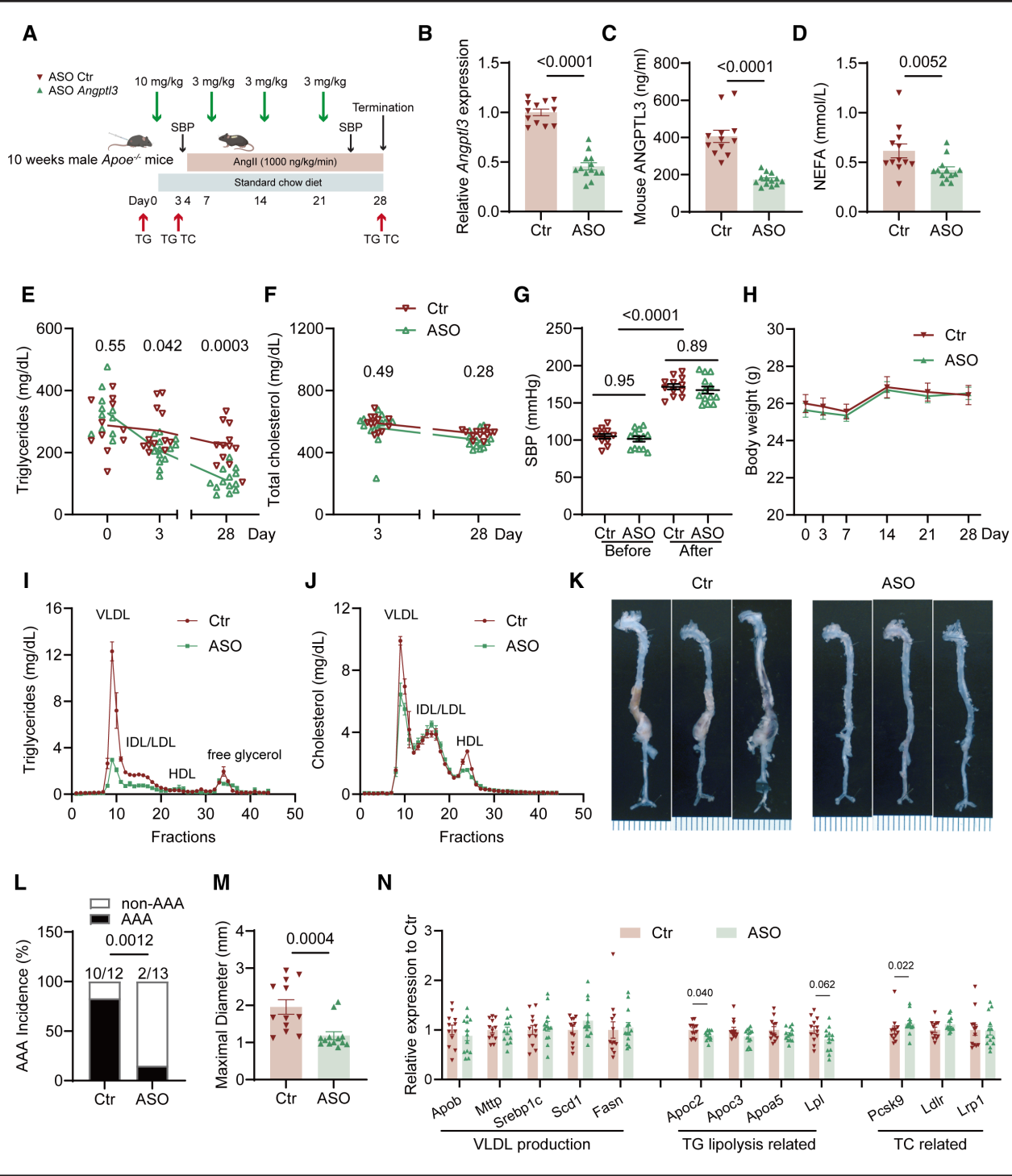


Figure 7. Administration of *Angptl3* antisense oligonucleotide prevents abdominal aortic aneurysm formation in *Apoe*-deficient mice.

A, Design of *Angptl3* antisense oligonucleotide study in male *Apoe*-deficient mice. Ten-week-old male *Apoe*-deficient mice were given a subcutaneous injection of the *Angptl3* antisense oligonucleotide (10 mg/kg, n=14 in the beginning and 13 at the end point) or scrambled antisense oligonucleotide (n=14 in the beginning and 12 at the end point). After 3 days, mice were infused with angiotensin II (1000 ng/kg/min) for 25 days. Three more injections were administered on days 7, 14, and 21. At the end of the study, aortas, livers, and plasma were harvested.

B, Relative abundance of *Angptl3* mRNA in the liver. **C** and **D**, Plasma ANGPTL3 protein concentrations (**C**) and nonesterified fatty acids (**D**) at the end point. **E**, Plasma triglyceride levels on days 0, 3, and 28. **F**, Plasma total cholesterol concentrations on days 3 and 28. **G**, Systolic blood pressure before and after angiotensin II infusion. **H**, Body weight changes. **I** and **J**, triglyceride (**I**) and cholesterol (**J**) concentrations of size exclusion chromatography fractionated plasma from animals (n=4 in the control group, n=4 in the *Angptl3* antisense oligonucleotide group) were determined by enzymatic assays. Fractions 8 to 11 contained very low-density lipoprotein, fractions 12 to 17 contained (Continued)

Figure 7 Continued. intermediate-density lipoprotein and low-density lipoprotein, and fractions 22 to 25 contained high-density lipoprotein.

K, Representative aortic images from the 2 groups. **L** and **M**, Quantification of abdominal aortic aneurysm incidence (**L**) and maximal aortic diameter (**M**). **N**, Relative liver mRNA abundance of genes related to very low-density lipoprotein production (*Apol*, *Mtp*, *Srebp1c*, *Scd*, and *Fasn*), triglyceride lipolysis (*Apoc2*, *Apoc3*, *Apoa5*, and *Lpl*), and TC regulation (*Pcsk9*, *Ldlr*, and *Lrp1*). Data are presented as circles/dots or mean \pm SEM. Statistical analyses were conducted as follows: Student *t* test for **B** and **C**; Mann-Whitney *U* test for **D** and **M**; 2-way mixed-effects ANOVA followed by Sidak post hoc analysis for **E** through **G**; Fisher exact test for **L**; and Student *t* test or Mann-Whitney *U* test for **N**. Scale bars=1 mm (each interval) in **K**. AAA indicates abdominal aortic aneurysm; ASO, antisense oligonucleotide; Ctr, control; HDL, high-density lipoprotein; IDL, intermediate-density lipoprotein; LDL, low-density lipoprotein; NEFA, non-esterified fatty acid; SBP, systolic blood pressure; TC, total cholesterol; TG, triglyceride; and VLDL, very low-density lipoprotein.

function mutant of PCSK9, in which *Ldlr*-deficient mice and PCSK9-overexpressing mice are fed a Western diet to augment hypercholesterolemia.²⁶ Compared with C57BL/6J mice, *Ldlr*- or *Apoe*-deficient mice have significantly increased TC and TG concentrations, which are predominantly found in VLDL fractions using size exclusion chromatography to separate lipoprotein classes,⁴¹ indicating that increased concentrations of large, TG-rich lipoproteins are associated with AAA formation. Our previous study demonstrated that AAA development is accelerated with modestly hypercholesterolemic conditions, but further elevation of cholesterol above a threshold level does not enhance AAA progression.⁴⁰ Here, using 3 hypertriglyceridemia mouse models, we show that increased TG concentrations contribute to AAA development, dissection, and rupture in a TG concentration-dependent manner (Table S7). The moderately increased TG concentrations in *Apoa5* deficient mice accelerated AAA development, dramatically increased TG concentrations in hAPOC3 Tg mice caused AAA dissection, and severely high TG concentrations resulted in aortic rupture and death in *iLpf*^{-/-} mice. We also evaluated the effects of increased TG concentrations on aneurysm growth in the elastase-induced AAA model. Previous studies using C57BL/6J mice with PCSK9 OE or *Apoe*-deficient mice have demonstrated that the aneurysm growth in the PPE model is independent of hypercholesterolemic conditions.^{27,42} Using the PPE-induced AAA model, we demonstrated that increased TG concentrations aggravated AAA growth in both male and female hAPOC3 Tg mice. Furthermore, clinical observation shows that plasma TG concentrations are higher in patients with AAA than in controls.⁹ In a prospective epidemiological study (the BUPA study [British United Provident Association]), the risk of death from AAA rupture is strongly related to serum TG concentrations.¹⁰ Together, these findings pave the way for future studies of the role of TGs and related metabolites in AAA development.

Importantly, our study demonstrates that lowering TG and NEFA levels by administering the *Angptl3* ASO inhibits AAA development in both hAPOC3 Tg mice and *Apoe*-deficient mice. ApoC-III raises TG concentrations by inhibiting LPL activity, reducing hepatic uptake of TG-rich lipoproteins, and promoting VLDL secretion. ApoE acts as a critical ligand for the LDL receptor and the LDL receptor-related protein, facilitating the uptake of chylo-

micron and VLDL remnants into hepatocytes. Deficiency of ApoE causes elevated TG and TC levels. In both *APOC3* Tg mice and *Apoe*-deficient mice, TGs and cholesterol are mainly distributed in VLDL fractions. Administration of *Angptl3* ASO dramatically reduced TG levels in VLDL and intermediate-density lipoprotein fractions, consistent with decreased TG concentrations in plasma, supporting the hypothesis that large-sized TG-rich lipoproteins and related metabolites contribute to AAA progression and rupture. These findings also provide evidence that lowering TG-rich lipoproteins is a potential therapeutic strategy. ANGPTL8 and ANGPTL3 form a complex that markedly inhibits LPL activity. Similar to the effects of the *Angptl3* ASO on AAA, *Angptl8* deficiency or knockdown reduced AAA formation by lowering TG concentrations and suppressing the inflammatory response in *Apoe*-deficient mice.⁴³ Administration of fenofibrate also reduced the severity of experimental AAA in *Ldlr*- and *Apoe*-deficient mice.^{44,45} However, fenofibrate did not significantly limit AAA growth in patients with AAA in FAME-2 (Fenofibrate in the Management of Abdominal Aortic Aneurysm 2), a placebo-controlled clinical trial.⁴⁶ We should note that it may take an estimated 5 years for a small AAA with a diameter of 40 to 55 mm to reach 55 mm, the size threshold for intervention.³⁹ In the FAME-2 study, AAA diameters in the control group increased only about 1 mm after a 24-week observation period, making it hard to determine the effects of fenofibrate. Additionally, AAA diameters in the 2 groups began to diverge at the end of the evaluation, suggesting that a long-term clinical trial with a larger sample size is needed to carefully assess the effects of TG lowering on AAA growth and rupture. Statins primarily target TC but also have a moderate TG-lowering effect (10% to 30%), depending on the statin type and dose. Although observational studies have found potential benefits of statins in AAA management by reducing inflammation, stabilizing the aortic wall, and lowering TC and TG levels, their impact on AAA growth and rupture risk remains controversial and inconclusive.⁴⁷⁻⁴⁹ This variability may be influenced by differences in statin types, dosages, and genetic metabolism-related factors. Therefore, high-quality randomized controlled trials are needed to clarify their role in AAA prevention and treatment.

AAA is characterized by pathological remodeling of the aortic ECM, including elastolysis and collagenolysis.

LOX is a crucial enzyme involved in the cross-linking of collagen and elastin in the ECM to maintain the structural integrity of the aortic wall. Impairments in LOX activity because of genetic mutations can lead to connective tissue disorders and promote aorta dissection.⁵⁰ *Lox*-deficient mice exhibit severe defects in vascular development, leading to perinatal death from aortic aneurysm.³² β-Aminopropionitrile is a well-known inhibitor of LOX and has been used extensively in research to accelerate AAA formation and rupture.⁵¹ LOX is initially synthesized as a preproprotein and secreted into the extracellular space, where the prolysyl oxidase is cleaved by proteases, including BMP-1, ADAMTS2, and ADAMTS14. Increased TG concentrations or the presence of palmitate dramatically blocked LOX maturation and reduced LOX activity in aortas and HASMCs. Based on RNA-seq findings, *BMP1* and *ADAMTS2* are highly abundant in HASMCs. PA downregulated the expression of *BMP1* and *ADAMTS2*, causing decreased LOX maturation. In this study, we confirmed that BMP-1 is the predominant enzyme regulating LOX maturation in HASMCs. The increase in LOX transcription upon *BMP1* knockdown or palmitate treatment was likely a compensatory response; however, it was insufficient to compensate for the loss of mature LOX. Increasing the substrate availability through LOX OE could partially compensate for reduced BMP-1 function and produce a certain amount of mature LOX. Further analysis of liver-aorta crosstalk using data from the Genotype-Tissue Expression project revealed that the liver is predicted to influence aortic gene expression through the secretion of APOC3. Notably, higher liver *APOC3* levels are associated with lower *BMP1* expression in the aorta. Previous studies have shown that LOX OE can inhibit AAA development in the CaCl₂-induced AAA model.⁵² In our AngII model in h*APOC3*Tg mice, local LOX OE in the suprarenal aorta completely abolished the effects of high TG on promoting suprarenal AAA. Additionally, PA induces vascular smooth muscle cell apoptosis, promotes inflammatory responses, enhances oxidative stress, and triggers proliferation and migration, contributing to the progression of vascular diseases such as atherosclerosis and hypertension.⁵³ In this study, we demonstrated that PA, as a metabolite of plasma TGs or endogenously synthesized in the liver, may contribute to AAA development by inhibiting LOX maturation. These findings uncover a novel liver-aorta regulatory mechanism in which APOC3-induced hypertriglyceridemia suppresses BMP-1 and impairs LOX maturation and activity, potentially driving AAA formation.

Plasma TG concentrations include the content of various lipoprotein particles. Multiple genes, such as LPL, APOC3, APOC2, APOA5, and ANGPTL3, influence TG metabolism and regulate plasma TG concentrations. Among them, APOC3 and ANGPTL3 are targets for drug development because loss-of-function mutations in APOC3 and ANGPTL3 are associated with improved

lipid profiles and reduced cardiovascular risk. Preclinical and clinical data have well documented that ApoC-III or ANGPTL3 inhibitors effectively reduce severe hypertriglyceridemia. These inhibitors include ASOs,^{14,16,37} monoclonal antibodies,⁵⁴ small interfering RNA,^{55,56} and CRISPR-Cas (clustered regularly interspaced short palindromic repeats [CRISPR] and associated proteins [Cas]) gene editing strategies.^{57,58} Preclinical and clinical data have demonstrated that ANGPTL3 inhibitors are highly effective for treating severe hypertriglyceridemia by upregulating LPL activity and facilitating the hydrolysis and clearance of TG-rich lipoproteins. As h*APOC3*Tg mice have very high APOC3 and TG concentrations, the *Angptl3* ASO was administered at 50 mg/kg per week in previous studies.¹⁶ In this study, administration of an *Angptl3* ASO at a much lower dosage effectively reduced AAA development in h*APOC3*Tg mice and *Apoe*-deficient mice by reducing TG concentrations, especially TG concentrations in VLDL fractions. We observed that administration of the *Angptl3* ASO mainly decreased plasma TG concentrations, with a limited reduction in plasma TC concentrations in h*APOC3*Tg mice. In *Apoe*-deficient mice, administration of the *Angptl3* ASO only reduced TG concentrations. These results further support the idea that managing TG-rich lipoprotein concentrations is a potential therapeutic strategy for treating AAA.

This study has several limitations. First, although our animal models exhibit increased TG levels, some also show concurrent alterations in TC levels, making it challenging to fully distinguish their independent effects. However, the strong correlation between TG levels and AAA severity, the mechanistic link between TG and LOX inhibition, and the therapeutic efficacy of TG-lowering strategies via *Angptl3* ASO administration collectively support a direct role of hypertriglyceridemia in AAA pathogenesis. Second, although we have identified the essential role of PA in regulating VSMC LOX maturation and activity, there is no direct evidence of increased PA uptake or accumulation in the aorta. Elevated circulating PA levels have been associated with an increased risk of major adverse cardiovascular events.⁵⁹ Ethyl palmitate is an esterified, lipid-soluble derivative of PA that facilitates efficient systemic delivery because it is rapidly hydrolyzed in vivo by endogenous esterases to release free PA.³⁶ Considering that ethyl palmitate differs structurally from free PA, future studies should explore the prognostic significance of PA levels in AAA and investigate the involvement and mechanisms of PA uptake and use in the diseased aorta. Finally, although the *Lpl* knock out mouse model provides valuable insights into the impact of severe TG elevation on AAA, its extreme hypertriglyceridemia limits translational relevance. To address this, we incorporated moderate hypertriglyceridemia models for mechanistic and therapeutic studies. *Lpl* knock out mice exhibit severely elevated TG

and chylomicron levels, closely mirroring human familial chylomicronemia syndrome, a rare and severe condition affecting approximately 1 in 1 000 000 individuals.⁶⁰ In contrast, heterozygous hAPOC3-Tg, Apoa5-deficient, and Apoe-deficient mice develop mild to moderate hypertriglyceridemia when fed a standard chow diet, resembling familial hypertriglyceridemia, a more common disorder affecting approximately 1 in 100 individuals.⁶¹ Future studies using animal models with selective modulation of TG, cholesterol, or TG-rich lipoprotein levels will be essential to clarify their distinct contributions to AAA pathogenesis and therapeutic targeting.

In summary, the present study, combined with recent genetic, proteomic, and metabolomic findings, indicates that increased TG concentrations contribute to an increased risk of AAA. Individuals with higher genetic predisposition for AAA may benefit from targeted interventions. Understanding the association between TG concentrations and AAA risk has important clinical implications. Notably, our results demonstrate that ASO therapy targeting liver ANGPTL3 holds potential as a therapeutic approach to reduce AAA risk. These findings underscore the need for additional experimental and clinical investigations into the mechanisms and therapeutic strategies for AAA treatment through TG-lowering therapies.

ARTICLE INFORMATION

Received March 23, 2025; accepted July 15, 2025.

Affiliations

Frankel Cardiovascular Center, Department of Internal Medicine (Y.L., H.W., Ying Zhao, Y.C., Y.D., Yang Zhao, X.W., G.Z., C.X., H. Liu, I.S., L.C., J.Z., Y.E.C., Y.G.) and Center for Advanced Models for Translational Sciences and Therapeutics (Y.E.C.), University of Michigan Medical Center, Ann Arbor. Department of Molecular Physiology and Biological Physics, University of Virginia School of Medicine, Charlottesville (H.W.). Department of Pharmacology, University of Michigan, Ann Arbor (M.Y., A.S.). Saha Cardiovascular Research Center and Department of Physiology, College of Medicine, University of Kentucky, Lexington (L.C., H.S.L., A.D., R.E.T.). Department of Pharmacology, Southern University of Science and Technology, Guangdong, China (H. Lu). College of Pharmacy Health, University of Houston, Houston, TX (G.Z.). Department of Internal Medicine, Rochester General Hospital, Rochester, NY (C.X.).

Sources of Funding

This study was partially supported by National Institutes of Health grants HL166203 (to Y.G.), HL165688 (to Y.G. and A.S.), HL109946 and HL134569 (to Y.E.C.), HL151524 (to L.C.), HL153710 (to J.Z.), HL172832 (to G.Z.), R35HL155649 (to A.D.), and UL1TR001998 (to R.E.T. and H.S.L.) and by American Heart Association Merit award 23MERIT1036341 (to A.D.) and postdoctoral fellowships 25POST1376587 (to Y.L.) and 24POST1196020 (to M.Y.).

Disclosures

None.

Supplemental Material

Supplemental Methods

Figures S1–S11

Tables S1–S7

References 62–87

Uncropped gel blots

ARRIVE checklist

REFERENCES

- Nordon IM, Hinchliffe RJ, Loftus IM, Thompson MM. Pathophysiology and epidemiology of abdominal aortic aneurysms. *Nat Rev Cardiol*. 2011;8:92–102. doi: 10.1038/nrcardio.2010.180
- The United Kingdom Small Aneurysm Trial Participants. Long-term outcomes of immediate repair compared with surveillance of small abdominal aortic aneurysms. *N Engl J Med*. 2002;346:1445–1452. doi: 10.1056/NEJMoa013527
- Soden PA, Zettervall SL, Ultee KH, Darling JD, Buck DB, Hile CN, Hamdan AD, Schermerhorn ML. Outcomes for symptomatic abdominal aortic aneurysms in the American College of Surgeons National Surgical Quality Improvement Program. *J Vasc Surg*. 2016;64:297–305. doi: 10.1016/j.jvs.2016.02.055
- Reimerink JJ, van der Laan MJ, Koelemeij MJ, Balm R, Legemate DA. Systematic review and meta-analysis of population-based mortality from ruptured abdominal aortic aneurysm. *Br J Surg*. 2013;100:1405–1413. doi: 10.1002/bjs.9235
- Golledge J, Thanigaimani S, Powell JT, Tsao PS. Pathogenesis and management of abdominal aortic aneurysm. *Eur Heart J*. 2023;44:2682–2697. doi: 10.1093/euroheartj/eahd386
- Roychowdhury T, Klarin D, Levin MG, Spin JM, Rhee YH, Deng A, Headley CA, Tsao NL, Gellatly C, Zubler V, et al; DiscovEHR. Genome-wide association meta-analysis identifies risk loci for abdominal aortic aneurysm and highlights PCSK9 as a therapeutic target. *Nat Genet*. 2023;55:1831–1842. doi: 10.1038/s41588-023-01510-y
- Harrison SC, Holmes MV, Burgess S, Asselbergs FW, Jones GT, Baas AF, van 't Hof FN, de Bakker PIW, Blankenstein JD, Powell JT, et al. Genetic association of lipids and lipid drug targets with abdominal aortic aneurysm: a meta-analysis. *JAMA Cardiol*. 2018;3:26–33. doi: 10.1001/jamacardio.2017.4293
- Klarin D, Damrauer SM, Cho K, Sun YV, Teslovich TM, Honerlaw J, Gagnon DR, DuVall SL, Li J, Peloso GM, et al. Genetics of blood lipids among ~300,000 multi-ethnic participants of the Million Veteran Program. *Nat Genet*. 2018;50:1514–1523. doi: 10.1038/s41588-018-0222-9
- Norrgard O, Angquist KA, Johnson O. Familial aortic aneurysms: serum concentrations of triglyceride, cholesterol, HDL-cholesterol and (VLDL + LDL)-cholesterol. *Br J Surg*. 1985;72:113–116. doi: 10.1002/bjs.1800720215
- Watt HC, Law MR, Wald NJ, Craig WY, Ledue TB, Haddow JE. Serum triglyceride: a possible risk factor for ruptured abdominal aortic aneurysm. *Int J Epidemiol*. 1998;27:949–952. doi: 10.1093/ije/27.6.949
- Subramanian S. Hypertriglyceridemia: pathophysiology, role of genetics, consequences, and treatment. In: K.R. Feingold, B. Anawalt, M.R. Blackman, A. Boyce, G. Chrousos, E. Corpas, W.W. de Herder, K. Dhatariya, K. Dungan, J. Hofland, S. Kalra, G. Kaltsas, N. Kapoor, C. Koch, P. Kopp, M. Korbonits, C.S. Kovacs, W. Kuohung, B. Laferriere, M. Levy, E.A. McGee, R. McLachlan, M. New, J. Purnell, R. Sahay, A.S. Shah, F. Singer, M.A. Sperling, C.A. Stratakis, D.L. Treince and D.P. Wilson, eds. *Endotext*, 2000.
- Pennacchio LA, Olivier M, Hubacek JA, Cohen JC, Cox DR, Fruchart JC, Krauss RM, Rubin EM. An apolipoprotein influencing triglycerides in humans and mice revealed by comparative sequencing. *Science*. 2001;294:169–173. doi: 10.1126/science.1064852
- Breckenridge WC, Little JA, Steiner G, Chow A, Poapst M. Hypertriglyceridemia associated with deficiency of apolipoprotein C-II. *N Engl J Med*. 1978;298:1265–1273. doi: 10.1056/NEJM197806082982301
- Witztum JL, Gaudet D, Freedman SD, Alexander VJ, Digenio A, Williams KR, Yang Q, Hughes SG, Geary RS, Arca M, et al. Volanesorsen and triglyceride levels in familial chylomicronemia syndrome. *N Engl J Med*. 2019;381:531–542. doi: 10.1056/NEJMoa1715944
- Bergmark BA, Marston NA, Prohaska TA, Alexander VJ, Zimmerman A, Moura FA, Murphy SA, Goodrich EL, Zhang S, Gaudet D, et al; Bridge-TIMI 73a Investigators. Olezarsen for hypertriglyceridemia in patients at high cardiovascular risk. *N Engl J Med*. 2024;390:1770–1780. doi: 10.1056/NEJMoa2402309
- Graham MJ, Lee RG, Brandt TA, Tai LJ, Fu W, Peralta R, Yu R, Hurh E, Paz E, McEvoy BW, et al. Cardiovascular and metabolic effects of ANGPTL3 antisense oligonucleotides. *N Engl J Med*. 2017;377:222–232. doi: 10.1056/NEJMoa1701329
- Rosenson RS, Gaudet D, Hegele RA, Ballantyne CM, Nicholls SJ, Lucas KJ, San Martin J, Zhou R, Muhsin M, Chang T, et al. Zodasiran, an RNAi therapeutic targeting ANGPTL3, for mixed hyperlipidemia. *N Engl J Med*. 2024;391:913–925. doi: 10.1056/NEJMoa2404147

18. Burgess S, Mason AM, Grant AJ, Slob EAW, Gkatzionis A, Zuber V, Patel A, Tian H, Liu C, Haynes WG, et al. Using genetic association data to guide drug discovery and development: review of methods and applications. *Am J Hum Genet.* 2023;110:195–214. doi: 10.1016/j.ajhg.2022.12.017
19. Gaziano L, Giambartolomei C, Pereira AC, Gaulton A, Posner DC, Swanson SA, Ho YL, Iyengar SK, Kosik NM, Vujkovic M, et al; VA Million Veteran Program COVID-19 Science Initiative. Actionable druggable genome-wide Mendelian randomization identifies repurposing opportunities for COVID-19. *Nat Med.* 2021;27:668–676. doi: 10.1038/s41591-021-01310-z
20. Karjalainen MK, Karthikeyan S, Oliver-Williams C, Sliz E, Allara E, Fung WT, Surendran P, Zhang W, Jousilahti P, Kristiansson K, et al; China Kadoorie Biobank Collaborative Group. Genome-wide characterization of circulating metabolic biomarkers. *Nature.* 2024;628:130–138. doi: 10.1038/s41586-024-07148-y
21. Ibrahim M, Thanigaimani S, Singh TP, Morris D, Golledge J. Systematic review and meta-analysis of Mendelian randomisation analyses of abdominal aortic aneurysms. *Int J Cardiol Heart Vasc.* 2021;35:100836. doi: 10.1016/j.ijcha.2021.100836
22. Raffort J, Lareyre F, Clement M, Hassen-Khodja R, Chinetti G, Mallat Z. Diabetes and aortic aneurysm: current state of the art. *Cardiovasc Res.* 2018;114:1702–1713. doi: 10.1093/cvr/cvy174
23. Daugherty A, Cassis L. Chronic angiotensin II infusion promotes atherosclerosis in low density lipoprotein receptor -/- mice. *Ann N Y Acad Sci.* 1999;892:108–118. doi: 10.1111/j.1749-6632.1999.tb07789.x
24. Daugherty A, Manning MW, Cassis LA. Angiotensin II promotes atherosclerotic lesions and aneurysms in apolipoprotein E-deficient mice. *J Clin Invest.* 2000;105:1605–1612. doi: 10.1172/JCI7818
25. Lu H, Howatt DA, Balakrishnan A, Graham MJ, Mullick AE, Daugherty A. Hypercholesterolemia induced by a PCSK9 gain-of-function mutation augments angiotensin II-induced abdominal aortic aneurysms in C57BL/6 mice: brief report. *Arterioscler Thromb Vasc Biol.* 2016;36:1753–1757. doi: 10.1161/ATVBAHA.116.307613
26. Sawada H, Lu HS, Cassis LA, Daugherty A. Twenty years of studying AngII (angiotensin II)-induced abdominal aortic pathologies in mice: continuing questions and challenges to provide insight into the human disease. *Arterioscler Thromb Vasc Biol.* 2022;42:277–288. doi: 10.1161/ATVBAHA.121.317058
27. Mularz J, Spin JM, Beck HC, Tha Thi ML, Wagenhauser MU, Rasmussen LM, Lindahl JS, Tsao PSC, Steffensen LB. Hyperlipidemia does not affect development of elastase-induced abdominal aortic aneurysm in mice. *Atherosclerosis.* 2020;311:73–83. doi: 10.1016/j.atherosclerosis.2020.08.012
28. Golledge J. Abdominal aortic aneurysm: update on pathogenesis and medical treatments. *Nat Rev Cardiol.* 2019;16:225–242. doi: 10.1038/s41569-018-0114-9
29. Wu JH, Lemaitre RN, Manichaikul A, Guan W, Tanaka T, Foy M, Kabagambe EK, Djousse L, Siscovick D, Fretts AM, et al. Genome-wide association study identifies novel loci associated with concentrations of four plasma phospholipid fatty acids in the de novo lipogenesis pathway: results from the Cohorts for Heart and Aging Research in Genomic Epidemiology (CHARGE) consortium. *Circ Cardiovasc Genet.* 2013;6:171–183. doi: 10.1161/CIRGENETICS.112.964619
30. Carta G, Murru E, Banni S, Manca C. Palmitic acid: physiological role, metabolism and nutritional implications. *Front Physiol.* 2017;8:902. doi: 10.3389/fphys.2017.00902
31. Staiclescu MC, Kim J, Mecham RP, Wagenseil JE. Mechanical behavior and matrisome gene expression in the aneurysm-prone thoracic aorta of newborn lysyl oxidase knockout mice. *Am J Physiol Heart Circ Physiol.* 2017;313:H446–H456. doi: 10.1152/ajpheart.00712.2016
32. Lee VS, Halabi CM, Hoffman EP, Carmichael N, Leshchiner I, Lian CG, Bierhals AJ, Vuzman D, Brigham Genomic M, Mecham RP, et al. Loss of function mutation in LOX causes thoracic aortic aneurysm and dissection in humans. *Proc Natl Acad Sci U S A.* 2016;113:8759–8764. doi: 10.1073/pnas.1601442113
33. Franklin MK, Sawada H, Ito S, Howatt DA, Amioka N, Liang CL, Zhang N, Graf DB, Moorlegren JJ, Katsumata Y, et al. β -Aminopropionitrile induces distinct pathologies in the ascending and descending thoracic aortic regions of mice. *Arterioscler Thromb Vasc Biol.* 2024;44:1555–1569. doi: 10.1161/ATVBAHA.123.320402
34. Rosell-García T, Paradela A, Bravo G, Dupont L, Bekhouche M, Colige A, Rodriguez-Pascual F. Differential cleavage of lysyl oxidase by the metalloproteinases BMP1 and ADAMTS2/14 regulates collagen binding through a tyrosine sulfate domain. *J Biol Chem.* 2019;294:11087–11100. doi: 10.1074/jbc.RA119.007806
35. Liu Y, Yu M, Wang H, Dorsey KH, Cheng Y, Zhao Y, Luo Y, Zhao G, Zhao Y, Lu H, et al. Restoring vascular smooth muscle cell mitochondrial function attenuates abdominal aortic aneurysm in mice. *Arterioscler Thromb Vasc Biol.* 2025;45:523–540. doi: 10.1161/ATVBAHA.124.321730
36. Eguchi K, Manabe I, Oishi-Tanaka Y, Ohsugi M, Kono N, Ogata F, Yagi N, Ohto U, Kimoto M, Miyake K, et al. Saturated fatty acid and TLR signaling link beta cell dysfunction and islet inflammation. *Cell Metab.* 2012;15:518–533. doi: 10.1016/j.cmet.2012.01.023
37. Bergmark BA, Marston NA, Bramson CR, Curto M, Ramos V, Jeune A, Kuder JF, Park JG, Murphy SA, Verma S, et al; TRANSLATE-TIMI 70 Investigators. Effect of upanorsen on non-high-density lipoprotein cholesterol levels in statin-treated patients with elevated cholesterol: TRANSLATE-TIMI 70. *Circulation.* 2022;145:1377–1386. doi: 10.1161/CIRCULATIONAHA.122.059266
38. Plump AS, Smith JD, Hayek T, Aalto-Setala K, Walsh A, Verstuyft JG, Rubin EM, Breslow JL. Severe hypercholesterolemia and atherosclerosis in apolipoprotein E-deficient mice created by homologous recombination in ES cells. *Cell.* 1992;71:343–353. doi: 10.1016/0092-8674(92)90362-g
39. Ulug P, Powell JT, Martinez MA, Ballard DJ, Filardo G. Surgery for small asymptomatic abdominal aortic aneurysms. *Cochrane Database Syst Rev.* 2020;7:CD001835. doi: 10.1002/14651858.CD001835.pub5
40. Liu J, Lu H, Howatt DA, Balakrishnan A, Moorlegren JJ, Sorci-Thomas M, Cassis LA, Daugherty A. Associations of ApoAI and ApoB-containing lipoproteins with AngII-induced abdominal aortic aneurysms in mice. *Arterioscler Thromb Vasc Biol.* 2015;35:1826–1834. doi: 10.1161/ATVBAHA.115.305482
41. Ishibashi S, Herz J, Maeda N, Goldstein JL, Brown MS. The two-receptor model of lipoprotein clearance: tests of the hypothesis in "knockout" mice lacking the low density lipoprotein receptor, apolipoprotein E, or both proteins. *Proc Natl Acad Sci U S A.* 1994;91:4431–4435. doi: 10.1073/pnas.91.10.4431
42. Ikezoe T, Shoji T, Guo J, Shen F, Lu HS, Daugherty A, Nunokawa M, Kubota H, Miyata M, Xu B, et al. No effect of hypercholesterolemia on elastase-induced experimental abdominal aortic aneurysm progression. *Biomolecules.* 2021;11:1434. doi: 10.3390/biom11101434
43. Yu H, Jiao X, Yang Y, Lv Q, Du Z, Li L, Hu C, Du Y, Zhang J, Li F, et al. ANGPTL8 deletion attenuates abdominal aortic aneurysm formation in ApoE-/- mice. *Clin Sci (Lond).* 2023;137:979–993. doi: 10.1042/CS20230031
44. Krishna SM, Seto SW, Moxon JV, Rush C, Walker PJ, Norman PE, Golledge J. Fenofibrate increases high-density lipoprotein and sphingosine 1 phosphate concentrations limiting abdominal aortic aneurysm progression in a mouse model. *Am J Pathol.* 2012;181:706–718. doi: 10.1016/j.ajpath.2012.04.015
45. Golledge J, Cullen B, Rush C, Moran CS, Secomb E, Wood F, Daugherty A, Campbell JH, Norman PE. Peroxisome proliferator-activated receptor ligands reduce aortic dilatation in a mouse model of aortic aneurysm. *Atherosclerosis.* 2010;210:51–56. doi: 10.1016/j.atherosclerosis.2009.10.027
46. Pinchbeck JL, Moxon JV, Rowbotham SE, Bourke M, Lazzaroni S, Morton SK, Matthews EO, Hendy K, Jones RE, Bourke B, et al. Randomized placebo-controlled trial assessing the effect of 24-week fenofibrate therapy on circulating markers of abdominal aortic aneurysm: outcomes from the FAME -2 trial. *J Am Heart Assoc.* 2018;7:e009866. doi: 10.1161/JAHA.118.009866
47. Hosseini A, Sahranavard T, Reiner Z, Jamialahmadi T, Dhaheri YA, Eid AH, Sahebkar A. Effect of statins on abdominal aortic aneurysm. *Eur J Pharm Sci.* 2022;178:106284. doi: 10.1016/j.ejps.2022.106284
48. Takagi H, Yamamoto H, Iwata K, Goto S, Umemoto T; ALICE (All-Literature Investigation of Cardiovascular Evidence) Group. Effects of statin therapy on abdominal aortic aneurysm growth: a meta-analysis and meta-regression of observational comparative studies. *Eur J Vasc Endovasc Surg.* 2012;44:287–292. doi: 10.1016/j.ejvs.2012.06.021
49. Salata K, Syed M, Hussain MA, de Mestral C, Greco E, Mamdani M, Tu JV, Forbes TL, Bhatt DL, Verma S, et al. Statins reduce abdominal aortic aneurysm growth, rupture, and perioperative mortality: a systematic review and meta-analysis. *J Am Heart Assoc.* 2018;7:e008657. doi: 10.1161/JAHA.118.008657
50. Guo DC, Regalado ES, Gong L, Duan X, Santos-Cortez RL, Arnaud P, Ren Z, Cai B, Hostetler EM, Moran R, et al; University of Washington Center for Mendelian Genomics. LOX mutations predispose to thoracic aortic aneurysms and dissections. *Circ Res.* 2016;118:928–934. doi: 10.1161/CIRCRESAHA.115.307130
51. Kanematsu Y, Kanematsu M, Kurihara C, Tsou TL, Nuki Y, Liang EI, Makino H, Hashimoto T. Pharmacologically induced thoracic and abdominal aortic aneurysms in mice. *Hypertension.* 2010;55:1267–1274. doi: 10.1161/HYPERTENSIONAHA.109.140558

52. Yoshimura K, Aoki H, Ikeda Y, Fujii K, Akiyama N, Furutani A, Hoshii Y, Tanaka N, Ricci R, Ishihara T, et al. Regression of abdominal aortic aneurysm by inhibition of c-Jun N-terminal kinase. *Nat Med.* 2005;11:1330–1338. doi: 10.1038/nm1335
53. Hu Y, Fan Y, Zhang C, Wang C. Palmitic acid inhibits vascular smooth muscle cell switch to synthetic phenotype via upregulation of miR-22 expression. *Aging (Albany NY)*. 2022;14:8046–8060. doi: 10.1863/aging.204334
54. Gaudet D, Greber-Platzer S, Reeskamp LF, Iannuzzo G, Rosenson RS, Saheb S, Stefanutti C, Stroes E, Wiegman A, Turner T, et al. Evinacumab in homozygous familial hypercholesterolemia: long-term safety and efficacy. *Eur Heart J*. 2024;45:2422–2434. doi: 10.1093/euroheartj/ehae325
55. Watts GF, Schwabe C, Scott R, Gladding PA, Sullivan D, Baker J, Clifton P, Hamilton J, Given B, Melquist S, et al. RNA interference targeting ANGPTL3 for triglyceride and cholesterol lowering: phase 1 basket trial cohorts. *Nat Med.* 2023;29:2216–2223. doi: 10.1038/s41591-023-02494-2
56. Gaudet D, Clifton P, Sullivan D, Baker J, Schwabe C, Thackray S, Scott R, Hamilton J, Given B, Melquist S, et al. RNA interference therapy targeting apolipoprotein C-III in hypertriglyceridemia. *NEJM Evid.* 2023;2:EVIDo2200325. doi: 10.1056/EVIDo2200325
57. Zha Y, Lu Y, Zhang T, Yan K, Zhuang W, Liang J, Cheng Y, Wang Y. CRISPR/Cas9-mediated knockout of APOC3 stabilizes plasma lipids and inhibits atherosclerosis in rabbits. *Lipids Health Dis.* 2021;20:180. doi: 10.1186/s12944-021-01605-7
58. Zuo Y, Zhang C, Zhou Y, Li H, Xiao W, Herzog RW, Xu J, Zhang J, Chen YE, Han R. Liver-specific in vivo base editing of Angptl3 via AAV delivery efficiently lowers blood lipid levels in mice. *Cell Biosci.* 2023;13:109. doi: 10.1186/s13578-023-01036-0
59. He Y, Li S, Jiang L, Wu K, Chen S, Su L, Liu C, Liu P, Luo W, Zhong S, et al. Palmitic acid accelerates endothelial cell injury and cardiovascular dysfunction via palmitoylation of PKM2. *Adv Sci (Weinh.)*. 2025;12:e2412895. doi: 10.1002/advs.202412895
60. Baass A, Paquette M, Bernard S, Hegele RA. Familial chylomicronemia syndrome: an under-recognized cause of severe hypertriglyceridaemia. *J Intern Med.* 2020;287:340–348. doi: 10.1111/joim.13016
61. Miller M, Stone NJ, Ballantyne C, Bittner V, Criqui MH, Ginsberg HN, Goldberg AC, Howard WJ, Jacobson MS, Kris-Etherton PM, et al; American Heart Association Clinical Lipidology, Thrombosis, and Prevention Committee of the Council on Nutrition, Physical Activity, and Metabolism. Triglycerides and cardiovascular disease: a scientific statement from the American Heart Association. *Circulation.* 2011;123:2292–2333. doi: 10.1161/CIR.0b013e3182160726
62. Zheng J, Haberland Y, Baird D, Walker V, Haycock PC, Hurle MR, Gutteridge A, Erola P, Liu Y, Luo S, et al. Phenome-wide Mendelian randomization mapping the influence of the plasma proteome on complex diseases. *Nat Genet.* 2020;52:1122–1131. doi: 10.1038/s41588-020-0682-6
63. Ning Z, Huang Y, Lu H, Zhou Y, Tu T, Ouyang F, Liu Y, Liu Q. Novel drug targets for atrial fibrillation identified through Mendelian randomization analysis of the blood proteome. *Cardiovasc Drugs Ther.* 2023;38:1215–1222. doi: 10.1007/s10557-023-07467-8
64. Sun BB, Maranville JC, Peters JE, Stacey D, Staley JR, Blackshaw J, Burgess S, Jiang T, Paige E, Surendran P, et al. Genomic atlas of the human plasma proteome. *Nature.* 2018;558:73–79. doi: 10.1038/s41586-018-0175-2
65. Suhre K, Arnold M, Bhagwat AM, Cotton RJ, Engelke R, Raffler J, Sarwath H, Thareja G, Wahl A, DeLisle RK, et al. Connecting genetic risk to disease end points through the human blood plasma proteome. *Nat Commun.* 2017;8:14357. doi: 10.1038/ncomms14357
66. Yao C, Chen G, Song C, Keefe J, Mendelson M, Huan T, Sun BB, Laser A, Maranville JC, Wu H, et al. Genome-wide mapping of plasma protein QTLs identifies putatively causal genes and pathways for cardiovascular disease. *Nat Commun.* 2018;9:3268. doi: 10.1038/s41467-018-05512-x
67. Folkersen L, Fauman E, Sabater-Lleal M, Strawbridge RJ, Fränberg M, Sennblad B, Baldassarre D, Veglia F, Humphries SE, Rauramaa R, et al; IMPROVE study group. Mapping of 79 loci for 83 plasma protein biomarkers in cardiovascular disease. *PLoS Genet.* 2017;13:e1006706. doi: 10.1371/journal.pgen.1006706
68. Emilsson V, Ilkov M, Lamb JR, Finkel N, Gudmundsson EF, Pitts R, Hoover H, Gudmundsdottir V, Hormann SR, Aspelund T, et al. Co-regulatory networks of human serum proteins link genetics to disease. *Science.* 2018;361:769–773. doi: 10.1126/science.aaq1327
69. Pietzner M, Wheeler E, Carrasco-Zanini J, Cortes A, Koprulu M, Wörheide MA, Oerton E, Cook J, Stewart ID, Kerrison ND, et al. Mapping the proteo-
- genomic convergence of human diseases. *Science.* 2021;374:eabj1541. doi: 10.1126/science.abj1541
70. Ferkingsstad E, Sulem P, Atlasson BA, Sveinbjornsson G, Magnusson MI, Styrnisdottir EL, Gunnarsdottir K, Helgason A, Oddsson A, Halldorsson BV, et al. Large-scale integration of the plasma proteome with genetics and disease. *Nat Genet.* 2021;53:1712–1721. doi: 10.1038/s41588-021-00978-w
71. Folkersen L, Gustafsson S, Wang O, Hansen DH, Hedman AK, Schork A, Page K, Zhernakova DV, Wu Y, Peters J, et al. Genomic and drug target evaluation of 90 cardiovascular proteins in 30,931 individuals. *Nat Metab.* 2020;2:1135–1148. doi: 10.1038/s42255-020-00287-2
72. Zhang J, Dutta D, Köttgen A, Tin A, Schlosser P, Grams ME, Harvey B, Yu B, Boerwinkle E, Coresh J, et al; CKDGen Consortium. Plasma proteome analyses in individuals of European and African ancestry identify cis-pQTLs and models for proteome-wide association studies. *Nat Genet.* 2022;54:593–602. doi: 10.1038/s41588-022-01051-w
73. Sun BB, Chiou J, Taylor M, Benner C, Hsu YH, Richardson TG, Surendran P, Mahajan A, Robins C, Vasquez-Grinnell SG, et al; Alnylam Human Genetics. Plasma proteomic associations with genetics and health in the UK Biobank. *Nature.* 2023;622:329–338. doi: 10.1038/s41586-023-06592-6
74. Burgess S, Small DS, Thompson SG. A review of instrumental variable estimators for Mendelian randomization. *Stat Methods Med Res.* 2017;26:2333–2355. doi: 10.1177/0962280215597579
75. Burgess S, Butterworth A, Thompson SG. Mendelian randomization analysis with multiple genetic variants using summarized data. *Genet Epidemiol.* 2013;37:658–665. doi: 10.1002/gepi.21758
76. Burgess S, Bowden J, Fall T, Ingelsson E, Thompson SG. Sensitivity analyses for robust causal inference from Mendelian randomization analyses with multiple genetic variants. *Epidemiology (Cambridge, Mass.)*. 2017;28:30–42. doi: 10.1097/EDE.00000000000000559
77. Zuber V, Colijn JM, Klaver C, Burgess S. Selecting likely causal risk factors from high-throughput experiments using multivariable Mendelian randomization. *Nat Commun.* 2020;11:29. doi: 10.1038/s41467-019-13870-3
78. Willer CJ, Schmidt EM, Sengupta S, Peloso GM, Gustafsson S, Kanoni S, Ganna A, Chen J, Buchkovich ML, Mora S, et al; Global Lipids Genetics Consortium. Discovery and refinement of loci associated with lipid levels. *Nat Genet.* 2013;45:1274–1283. doi: 10.1038/ng.2797
79. Bycroft C, Freeman C, Petkova D, Band G, Elliott LT, Sharp K, Motyer A, Vukcevic D, Delaneau O, O’Connell J, et al. The UK Biobank resource with deep phenotyping and genomic data. *Nature.* 2018;562:203–209. doi: 10.1038/s41586-018-0579-z
80. Ala-Korpela M, Zhao S, Järvelin MR, Mäkinen VP, Ohukainen P. Apt interpretation of comprehensive lipoprotein data in large-scale epidemiology: disclosure of fundamental structural and metabolic relationships. *Int J Epidemiol.* 2022;51:996–1011. doi: 10.1093/ije/dyab156
81. Bharadwaj KG, Hiyama Y, Hu Y, Huggins LA, Ramakrishnan R, Abumrad NA, Shulman GI, Blaner WS, Goldberg IJ. Chylomicron- and VLDL-derived lipids enter the heart through different pathways: in vivo evidence for receptor- and non-receptor-mediated fatty acid uptake. *J Biol Chem.* 2010;285:37976–37986. doi: 10.1074/jbc.M110.174458
82. Trachet B, Aslanidou L, Piersigilli A, Fraga-Silva RA, Sordet-Dessimoz J, Villanueva-Perez P, Stampanoni MFM, Stergiopoulos N, Segers P. Angiotensin II infusion into ApoE-/- mice: a model for aortic dissection rather than abdominal aortic aneurysm? *Cardiovasc Res.* 2017;113:1230–1242. doi: 10.1093/cvr/cvx128
83. Xue C, Zhao G, Zhao Y, Chen YE, Zhang J. Mouse abdominal aortic aneurysm model induced by perivascular application of elastase. *J Vis Exp.* 2022; doi: 10.3791/63608-v
84. Lu H, Sun J, Liang W, Chang Z, Rom O, Zhao Y, Zhao G, Xiong W, Wang H, Zhu T, et al. Cyclodextrin prevents abdominal aortic aneurysm via activation of vascular smooth muscle cell transcription factor EB. *Circulation.* 2020;142:483–498. doi: 10.1161/CIRCULATIONAHA.119.044803
85. Shen H, Eguchi K, Kono N, Fujiw K, Matsumoto S, Shibata M, Oishi-Tanaka Y, Komuro I, Arai H, Nagai R, et al. Saturated fatty acid palmitate aggravates neointima formation by promoting smooth muscle phenotypic modulation. *Arterioscler Thromb Vasc Biol.* 2013;33:2596–2607. doi: 10.1161/ATVBAHA.113.302099
86. Love MI, Huber W, Anders S. Moderated estimation of fold change and dispersion for RNA-seq data with DESeq2. *Genome Biol.* 2014;15:550. doi: 10.1186/s13059-014-0550-8
87. Wu T, Hu E, Xu S, Chen M, Guo P, Dai Z, Feng T, Zhou L, Tang W, Zhan L, et al. clusterProfiler 4.0: A universal enrichment tool for interpreting omics data. *Innovation (Camb).* 2021;2:100141. doi: 10.1016/j.xinn.2021.100141